Alma Mater Studiorum – Università di Bologna

SCUOLA DI SCIENZE
Dipartimento di Chimica Industriale“Toso Montanari”

Corso di Laurea Magistrale in
Chimica Industriale

Classe LM-71- Scienze e Tecnologie della Chimica Industriale

Machine Learning Approach for Lowest Transition State Research of High Number Degrees of Freedom Homogeneous Catalysts

Tesi di Laurea Sperimentale

CANDIDATO

Giuseppe Cirillo

RELATORE

Chiar.mo Prof. Max Garcia-Melchor

Chiar.mo Prof. Marco Garavelli

CORRELATORE

Dott. Alessandro Lunghi

Anno Accademico 2020-2021

Abstract

Nowadays, interesting problems in computational chemistry are found in studying complex systems with a high number of degrees of freedom. Thus, is fundamental to provide a new way to handle them with a suitable tool capable of giving us the best compromise between accuracy and reliability using the minimum amount of computational time. In particular, these systems exhibit a high number of conformational isomers interconnected by low energy barriers and an accurate representation of their potential energy surface would allow us to identify the most stable isomer, the global minimum, and the transition state with the lowest energy. The challenge of this project is to provide a tool that helps us in this research, starting from a conformational analysis of four different homogeneous organocatalysts. This work aims to combine the Density Functional Theory accuracy and Molecular Mechanic Force Fields computational properties to explore the potential energy landscape using a Machine Learning approach.

COVID STATEMENT

Covid impacted the access to computational resources during this project, as access to some servers was limited from outside the College network. The main computational resources for this project were a local cluster based in trinity college and the supercomputer kay ICHEC's high-performance computer. The accessibility to the trinity college server was possible only from the campus itself or from another server called Rsync, which was down several times for periods of several days due to cooling system failure and updates. Also, since the restrictions were in observance during the period of my internship the queue of the clusters was really busy because everyone was home doing computational studies. The significant change due to covid restrictions was that all the meetings, training and project discussions had to move online, which was more challenging and different than normal face-to-face interactions. Unfortunately, after substantial work it was not possible to complete entirely the objectives set, but in spite of the general situation, good results had been provided with no major issues.

ACKNOWLEDGEMENTS

First of all, I would like to thank my supervisor, Max, for inspiring me to take on this project, guiding me through the entire realization of it, and Alessandro who gave me fundamental support during the implementation of his code. I would also thank Michael for his patients with all my questions and in particular for his help with the command terminals and scripts.

I would also thank Eric, Kevin, Manting and Arantxa for welcoming me into their group making me feel part of it.

Lastly, I would like to thank my family for their support during the quarantine.

Contents

Chapter 1. INTRODUCTION

1.1 The Importance of Conformational Search

Conformational diversity is an often neglected aspect in computational studies of transition metal complexes, especially when relatively large systems are involved. The number of conformers becomes difficult or impossible to manage by the only use of chemical intuition therefore an automated search need to be performed. In particular, the energy evaluation of a transition state (TS) is particularly challenging, since the different conformers may affect the stability of the transition state leading to a significant difference between the theoretical energy evaluation and the experimental data[1]. This effect becomes significant especially for molecules that contain transition metals, widely employed as a homogeneous catalyst for reactions such as C-C, C-N cross-coupling, and metathesis[2], where hindered and bulky ligands give the highest contribution to the conformation diversity. The challenge of this study is related to the almost infinite amount of transition states that define the Potential Energy Surface (PES) since the energy landscape is defined by 3N coordinates for each atom of the conformer. The computational cost for the evaluation of each TS is extremely prohibitive. A possible solution for this problem consists of the representation of the PES obtained by a conformational search, which allows us to explore a specific or wide portion of it. To simplify the manipulation of all these variables and reduce the computational cost at the minimum Molecular Mechanic Force Fields (MM-FF) are an extremely useful tool[3,4]. Recently, the use of this approach showed encouraging results at a really low computational cost although the accuracy of these methods is not always comparable with the deeper levels of theory. We propose with this work to combine the accuracy of DFT-level theory with a Molecular Mechanic Force Field to investigate and represent the PES. We wondered if it is possible to start only from one specific TS and run an automated conformational analysis carried out through a MM-FF to identify the key conformer, the lowest energy transition state, giving an accurate representation of the PES. In order to combine the DFT evaluation with the MM-FF

we use a Machine Learning approach (ML). ML is the study of computer algorithms that can improve automatically through experience and by the use of data. Given a specific mathematical model, such as a FF, it is possible to make predictions on the basis of a set of data specifically selected to improve the accuracy of the previsions. In recent years, machine learning has witnessed increasing attention as possibly evolutionary computational approaches. In particular, it has been demonstrated applicable to the prediction of complex potential energy surfaces through generalized regression methods. These methods have in common the fundamental feature of being able to represent a continuous function with no limitations with only an arbitrarily large number of parameters and a suitable representation of the atomic chemical environment.

1.2 High Degree Number Homogeneous Catalysts

For this work we focused on TSs with specific features to provide the best starting point for the conformational analysis; the criterion followed for this selection is based on two main features:

- a high number of degrees of freedom in terms of substituents' movements, such as torsions, rotations, and bending of bulky ligands.
- the presence of a high energy barrier for the TS formation.

The selection was carried out searching catalysts employed in reactions such as metathesis, C-C and C-N cross coupling previously investigated in the literature. The reason behind this choice is related to the high selectivity and specificity of these compounds toward chiral substrates due to the presence of bulky substituents as ligands, while the high activation barrier increases the possibility of finding different conformers with lower energy. At last, we have chosen catalysts which also presents experimental data to compare with our calculations.

1.2.1 $Pd(PPh_3)_2$ Catalysts

The first catalyst selected for this project is the $Pd(PPh_3)_2$, widely used for a large family of reactions such as Heck reaction, Suzuki coupling, Negishi coupling and other C-C cross coupling reactions in both industrial and research area[5,6]. The main property of this catalyst for this work derives from the presence of triphenylphospine bulky ligands which usually show the formation of the less hindered TS. This gives $Pd(PPh_3)_2$ a high specificity or selectivity throughout its typical reactions. The starting palladium complex is the *Tetrakis(Triphenylphosphine)palladium* $Pd[0](PPh_3)_4$, a saturate unreactive compound with 18 electrons in its electronic configuration. In solution, the dissociation of the ligands occur leading to the reactive specie $Pd[0](PPh_3)_2$, the respective unsaturated compound with 14 electrons in its electronic configuration. The presence of two empty *d* orbitals allows the complex to interact with other chemical species where the palladium reacts as an electron acceptor reaching saturation with four coordinated ligands. The majority of the ligands have alone pair of electrons in a filled sp^n type orbital that can overlap with the vacant *d*-orbital of Pd to form a conventional two-electron two-centre σ-bond, ligands of this type increase the electron density on the central metal atom. A bonding interaction is also possible between any filled *d* orbitals on the metal and the vacant ligand orbitals of appropriate symmetry such as π^* orbitals. This lead to a reduction of electron density on the metal in the known back-bonding, a common example is the coordination of CO to the complex. In spite of the lack of a potential lone pair or π-type orbital electrons, there is another class of ligands that can interact with the Palladium. This process usually occurs through the cleavage of a σ-bond in the reagent and the formation of two sigma-bonds between Pd and the ligands just formed. This process is known as oxidative addition. It occurs for a number of useful neutral species including hydrogen, carbon-hydrogen bonds and silanes as well as polarized bonds containing at last one electronegative atom such as aryl bromides. The product of this step contains an oxidized Pd(II) and two ligands bearing a formal negative charge.

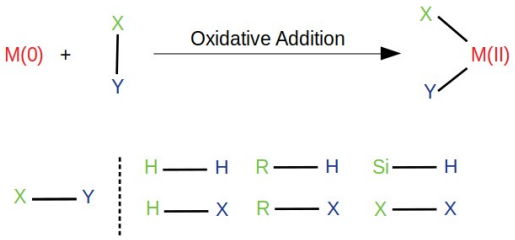

Figure -1.1. *General oxidative addition reaction for a metal complex M, halide X and reagent Y.*

Typically, the mechanism involved is a concerted reaction, where the X-Y σ-bond is broken and the new two σ-bonds are formed with the complex in just one step, without further intermediates, for this reason, the oxidative addition is often the rate-determining step of the reaction with the highest energy barrier along the reaction coordinate.

The transition state investigated for this project results from the oxidative addition of the PhenylBromide, *PhBr*, to the $Pd(PPh_3)_2$ from the work of Mcmullin *at ali*[7].

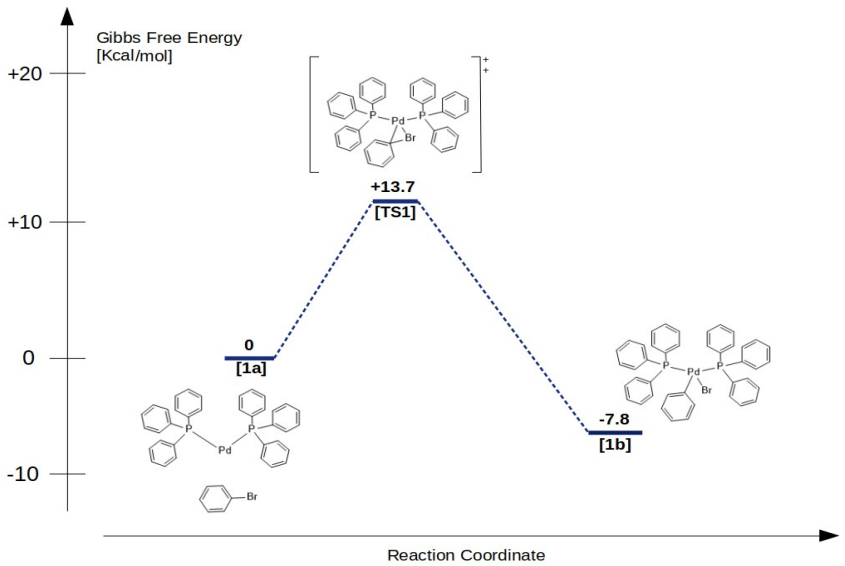

Figure-1.2. *Oxidative addition of PhBr to* $Pd(PPh_3)_2$

In this reaction mechanism, the bond broken is the aryl-halide in the structure **1a** while the two σ-bonds formed are respectively Pd-Ph and Pd-Br in **1b**. The energy cost of

this dissociation is compensated by the formation of two σ bonds resulting in a more stable product compared to the reagent. The reaction coordinate of this process is the cleavage of the C-Br bond, which, if sufficiently close to the palladium and well positioned, allows the formation of the **TS1**. In spite of the bulky PPh_3 ligands, the transition state is very flexible due to the possibility of the rotation of the ligands around the Pd-P bond as well as the six torsions around the P-Ph bonds, resulting in significant degrees of freedom for a wide energy range of several conformers.

1.2.2 PEPPSI Catalyst

Most reactions that occur around the transition metal are reversible and so the reverse of the oxidative addition, known as reductive elimination, provides a simple route for the release of neutral organic compounds from the complex. In this step, the ligands to be eliminated must be *cis* to one another for reductive elimination to occur. Since this reaction is reversible, when there is a choice the more stable product is formed, providing an extremely useful tool for regioselectivity reactions, in addition, this reaction also shows stereoselectivity since only the *syn* elimination is permitted allowing the retention of configuration, if any.

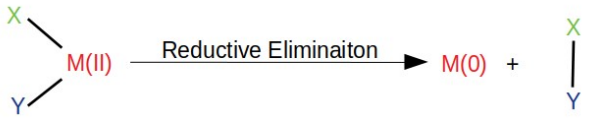

Figure-1.3*.Reductive elimination of a general metal M and reagents X and Y.*

As an example of reductive elimination, the second catalyst candidate is the PEPPSI (**p**yridine-**e**nhanced pre-catalyst **p**reparation **s**tabilization and **i**nitiation)[8], a Pd complex usually employed for C-N cross coupling such as Butchwald-Hartwig amination, Neghishi coupling and other cross coupling reactions. The Pd-complex can be used to promote nucleophilic substitution at vinylic or aromatic centres, for example, aromatic amines can be prepared directly from the corresponding bromides, iodides or triflates

and the required amine, in the presence of Pd(0) and a strong alkoxide base. The mechanism in this reaction mirrors that of coupling reactions. The first step, as usual, is the oxidative addition of Pd(0) into the aryl-halogen bond and the resulting complex Pd(II) adds the amine. The role of the base is to eliminate the halide from the complex allowing the reduction elimination to occur, forming a new Ar-N bond. The range of compounds can be various: both electron-withdrawing and electron-donating substituents are acceptable; hindered compounds or also acidic compounds are tolerated. The specific catalyst we have chosen is Pd-PEPPSI-(IPr$^{(OMe)}$*Ipr)^{An}, employed for a Buchwald-Hartwig amination between phenyl chloride, *PhCl*, and Aniline, $PhNH_2$, with the formation of a new C-N bond in the resulting diphenylamine as the final product[9], as shown in figure 1.4.

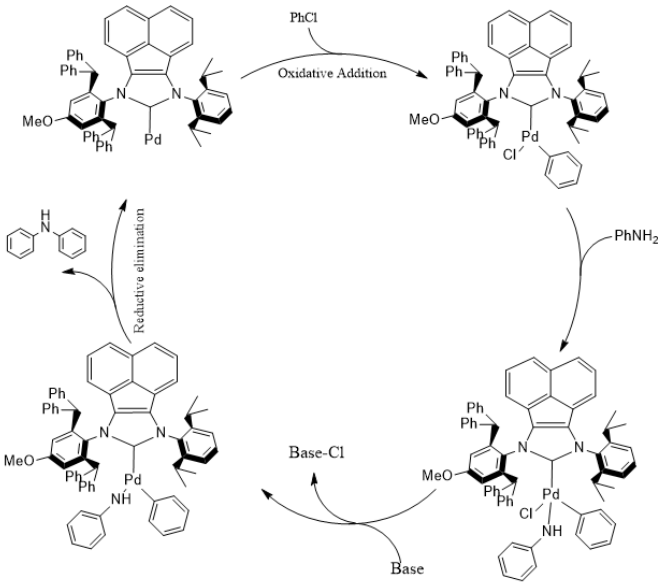

***Figure-1.4**. Buchwald-Hartwig amination scheme between phenyl chloride and aniline with PEPPSI catalyst*.

In the reaction coordinate of the theoretical study carried out by Xiao-Bing Lan *et ali*[9] we chose to investigate the transition state related to the reductive elimination step the due to the high energy barrier. The reaction step is here reported.

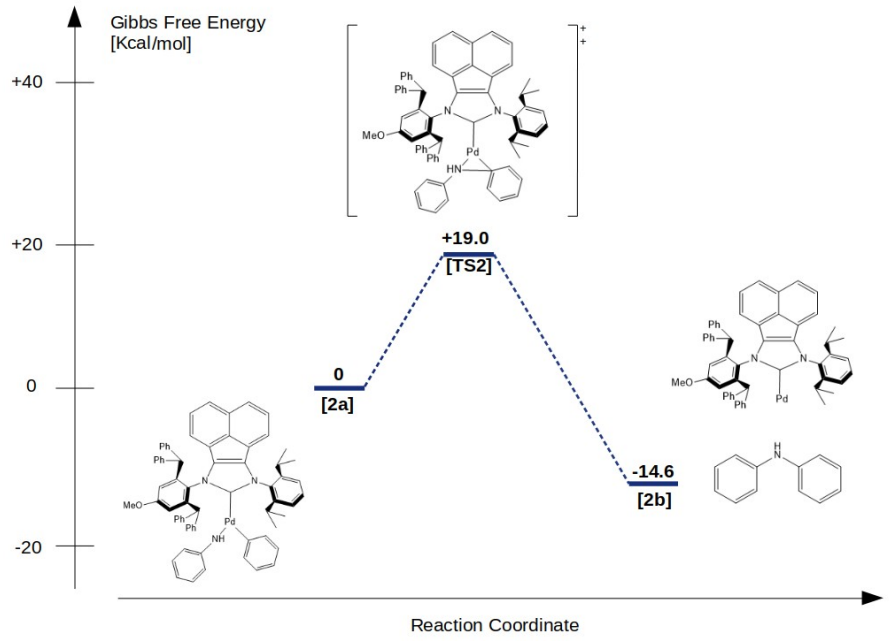

***Figure-1.5**. Reductive elimination of Diphenylamine from PEPPSI catalyst.*

As for the oxidative addition, the reductive elimination usually involves a concerted mechanism, in this case, the reaction coordinate is the formation of the new Ar-N bond allowing the formation of **2b** with the dissociation of the diphenylamine from the catalyst with an energy barrier of 19.0 Kcal/mol.

The **TS2** exhibit the highest number of degrees of freedom among all the catalysts selected for this project, in particular all the possible torsions of the substituents bonded to the two nitrogen atoms and the torsion of the Pd-carbene bond, with the drawback of having the N-heterocyclic skeleton of the structure unable to move due to its rigidity. Rigid and bulky catalysts are often neglected in wide conformational studies due to their low flexibility which commonly implies that the energy of transition states, such as **TS2,** are energetically highly susceptible even to short bond rotations, giving us the chance to test the reliability of the MM-FF fitting.

1.2.3 Grubbs II Catalysts

In 2005 the Nobel prize in chemistry was awarded jointly to Yves Chauvin, Robert H. Grubbs and Richard R. Schrock[10] for the development of the metathesis method in organic synthesis, an organic reaction that entails the redistribution of fragments of alkenes (olefin) by the scission and regeneration of carbon-carbon double bonds carried out using a carbene-Ru complex. Carbenes are neutral species containing a carbon atom with only six valence electrons, usually derived by photolysis of diazo-compounds, hydrogen alpha-elimination of compounds such chloroform or from the cationic dehydrogenation of imidazolium. The carbon atom in the carbene is reactive towards transition metal since a lone pair can be donated to the empty *d* orbital of metals such as ruthenium. These complexes are among the most important carbene-derived reagents since they are employed in alkene or olefin ring closing metathesis or cross metathesis reactions. The reaction involves the carbene complex addition to the alkene in a reversible [2+2] cycloaddition to give a four membered ring with the metal atom in the ring, the intermediate is known as "metallacyclobutane". The same reaction happens in reverse giving the same starting product or can continue by the cleavage of the other two sigma-bonds resulting in the formation of a new carbene complex with the same reactivity of the starting complex. The latter intermediate can now react in a second [2+2] cycloaddition with other alkenes with the formation of a new metallacyclobutane intermediate leading to the final product of the reaction. The two vinylic groups can belong to the same molecule or to different molecules, thus both intramolecular or intermolecular metathesis are allowed, the first resulting in a process known as ring close metathesis (RCM), the second resulting in a process known as cross metathesis.

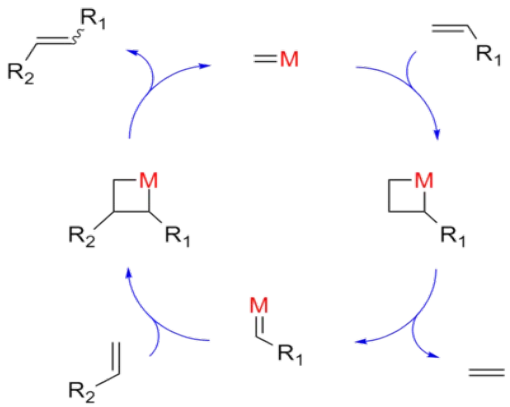

***Figure-1.6**. General metathesis reaction path.*

Through the years several ruthenium catalysts had been developed and, according to the type of ligands, they can be classified into different generations. First generation Grubbs I, which represents the precursor of all the other Grubbs-type catalysts is characterized by the presence of the metal Ru coordinated with two chlorine atoms, two PCy_3 ligands and a benzylidene. The second generation Grubbs II has the same use in organic synthesis as the first generation catalyst but generally with higher activity. It is characterized by the presence of a N-heterocyclic carbene, (1,3-bis(2,4,6-trimethylphenyl)imidazole), instead of one PCy_3 ligand which makes the catalyst particularly stable towards moisture and air. A further modification of the Grubbs II with the presence of chelating ligand, the ortho-isopropoxybenzylidene, instead of the PCy_3 and the benzylidene is commonly known as Hoveyda-Grubbs catalyst, leading to a phosphine-free structure resulting in a much more stable compound. The latter shows a slow initiation rate which can be balanced and modified by changing the steric and electronic properties of the chelate[11,12].

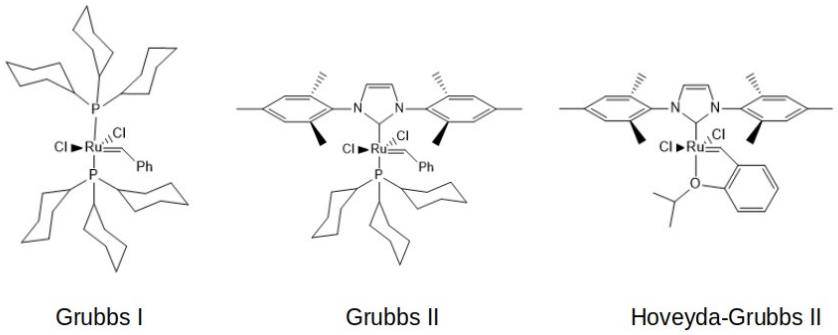

***Figure-1.7**. Well-defined ruthenium-base olefin metathesis catalysts.*

The transition state investigated in our work is the one identified in the metathesis reaction the addition of trichloridevinylsilane, $H_2CHCSiCl_3$ to the Grubbs II catalyst from the study of Śliwa et *ali*[13], as reported in the following figure.

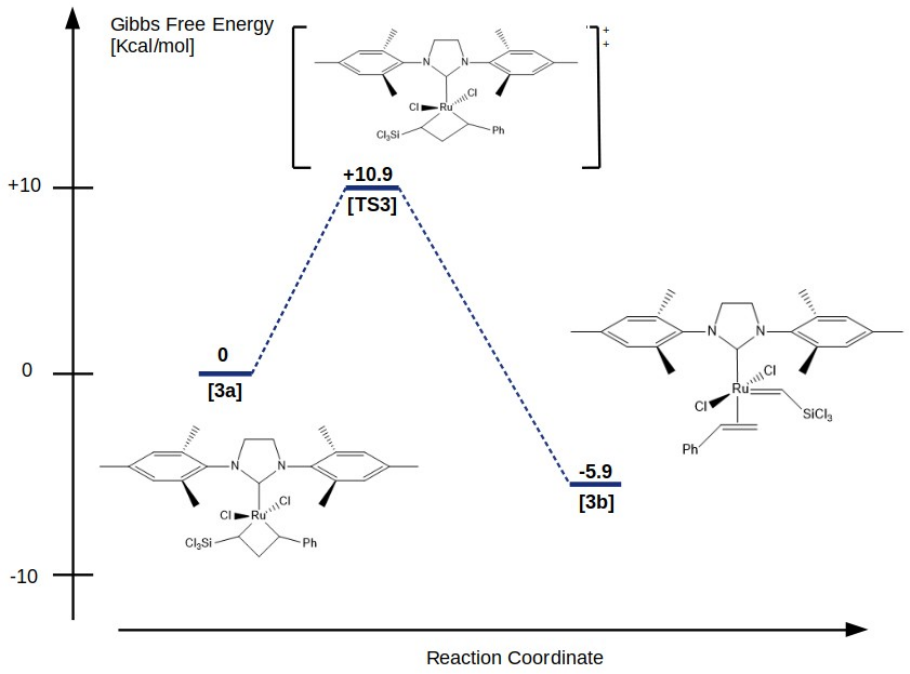

***Figure-1.8**. Metathesis reaction between Grubbs II and trichloridevinylsilane.*

The TS identified involves the cleavage of the H_2C-CSi and Ru-Cph bonds for the formation of a styrene molecule and the trichloridesilidene. The significant degrees of freedom of **TS3** are the two torsion of imidazolium's substituents and their methyl groups as well as the torsion around the Ru-Carbene bond.

1.2.4 Xantphos Catalysts

The last catalyst candidate is the Xantphos, a ruthenium-based complex chelated by the bidentate phosphine 4,5-bis-(diphenylphosphino)-9,9-dimethylxanthene, employed for its rigidity structure connected to four flexible phenyl groups which provide to the catalyst a certain flexibility, allowing it to react also with bulky substrates. As for the PEPPSI it is usually employed for Butchwald-Hartwig amination but several studies identified this catalyst as particularly promising for the Knoevenagel reaction[14,15], the conversion of oxide ethers into nitriles[16], for the synthesis of heterocyclic compounds[17] and hydroformylation of alkenes[18]. It is frequently employed in reactions that involves C-O bond cleavage as well as O-H groups bond cleavage to promote the formation of a ketone intermediate[19]. In particular, the TS we focused on for this catalyst involves the oxidative addition of the Ru-complex to the O-H bond of the 2-phenoxy-1-phenylethan-1-ol **4c** of the tandem alcohol dehydrogenation and reductive aryl-ether cleavage from the study of Chmely e*t ali*[20], reported in figure 1.9. The oxidative addition follows the same principle explained in the previous chapter for the $Pd(PPh_3)_2$ catalyst, with the only difference that the coordination between the oxygen atom and the Ruthenium complex is preferred **4a**, followed by the oxidative addition of both atoms, hydrogen and oxygen to the ruthenium with the formation of two σ bonds. The degrees of freedom we are interested in are the very flexible torsions of the four phenyl groups connected to the rigid part of the catalyst.

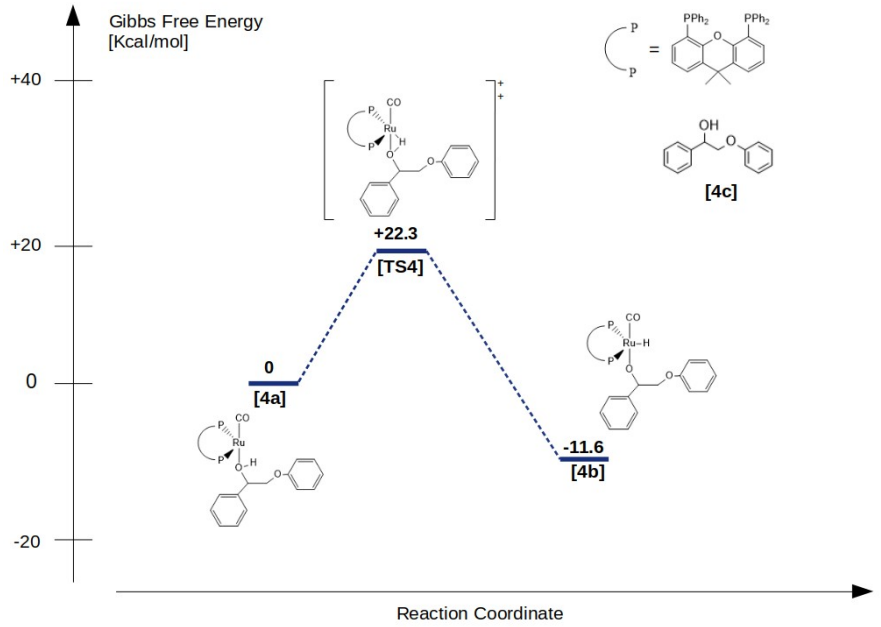

Figure – 1.9. *Oxidative addition of 2-phenoxy-1-phenylethan-1-ol to Xantphos*

1.3 Objectives

The main objective of this work is to provide a framework for an automated transition state research of bulky ligands. To fulfill this purpose we aim to parameterize a Molecular Mechanic Force Field in combination with a Machine Learning approach to run an automated conformational search in a Molecular Dynamic environment with the purpose of exploring the potential energy landscape of several catalysts with the same accuracy of DFT calculations. To succeed in the objective a crucial step is the identification of the starting conformers to generate a reliable training set for the force field parametrization. Here we provide a starting conformational search with the help of Macromodel as provided by Schrödinger Maestro demo software followed by cluster analysis in order to classify the conformers in different families, lowering the number of structures for the MM-FF fitting while preserving the conformational variety.

Chapter 2. THEORETICAL PRINCIPLES

2.1 Density Functional Theory

Many different methods exist for calculating the electronic structures and properties of atomic systems. A large hierarchy of methods allows us to provide a very accurate answer. However, the most accurate calculations are often computationally prohibitive in terms of cost. A solution for this problem is using Density Functional Theory (DFT) which provides a good balance between accuracy and computational cost for ground state electronic structures of molecules. It describes the quantum behavior through a functional of electronic density which depends only on three spatial coordinates, simplifying the representation of the wave function. The theoretical foundation of a general chemical system can be described by the Schrödinger equation shown in Eq. 2.0.

$$-\sum_i \left(\frac{\hbar^2}{2m_e}\nabla_k^2\right)-\sum_i \left(\frac{\hbar^2}{2m_N}\nabla_k^2\right)-\sum_i\sum_k \left(\frac{e^2 Z_k}{r_{ik}}\right)+\sum_{i<j}\left(\frac{e^2}{r_{ij}}\right)+\sum_{k<l}\left(\frac{e^2 Z_k Z_l}{r_{kl}}\right)\Psi = E\Psi \qquad \text{Eq.2.0}$$

Where i and j run over electrons, k and l run over nuclei, Z is the nuclear atomic number, Ψ is the wave function and E is the eigenvalue which represents the energy of all the possible states of the system. The entire operator on the left is known as Hamiltonian operator $\hat{H}$. In the same order as shown, the different terms of the equation represent different components of the energy, electron kinetic energy, nuclei kinetic energy, electron-nuclei interaction, electron-electron interaction and nuclei-nuclei interaction. Since the exact solution of this equation is impossible to be found analytically for a many electron system, approximations are needed. The Born-Oppenheimer approximation[21] is the most important one, the key idea is to consider the position of the nucleus fixed respecting to the electrons' motion as the nucleus motion is way slower than the electron one, this lead to the possibility of neglecting the nuclei kinetic energy and considering the interaction between them as constant. Leading to the following equation.

$$\left(-\sum_i \left(\frac{\hbar^2}{2m_e}\nabla^2\right)-\sum_i\sum_k\left(\frac{e^2 Z_k}{r_{ik}}\right)+\sum_{i<j}\left(\frac{e^2}{r_{ij}}\right)\right)\Psi = E\Psi \qquad \text{Eq. 2.1}$$

Several theories and approaches has been developed in order to find an accurate definition of Ψ, but due to its simplicity and computational efficiency, DFT is the most widely used method to fulfill this purpose. It allows us to calculate meaningful physical properties through the computation of a functional expressed by the electron density. The first description of this theory was provided by the Thomas-Fermi equation under the approximations of non-interacting electrons and an infinite uniform electron gas (UEG)[22–24]. The energy functional is shown in the Eq. 2.2.

$$E[p(r)]=\frac{3}{10}\left(3\pi^2\right)^{\frac{2}{3}}\int \rho(r)^{\frac{5}{3}}dr-\sum_k\int\left(\frac{Z_k}{|r-R_k|}\rho(r)dr\right)+\frac{1}{2}\iint\left(\frac{\rho(r_1)\rho(r_2)}{r_{12}}dr_1 dr_2\right) \qquad \text{Eq. 2.2}$$

In this first approach, the energy description shows poor performances for realistic chemical systems due to the lack of electronic exchange and correlation and due to the assumption that the kinetic energy density functional cannot describe systems of non-uniform electron density.

2.1.1 Hohenberg-Kohn and Kohn-Sham Theorem

A very important improvement in the DFT was made by Hohenberg and Kohn, in their studies, two theorems can be considered as the main foundation of this method, the Hohenberg-Kohn theorem and the Kohn-Sham theorem.

The first proves that a non-degenerate ground state density of a system is uniquely described by a specific external potential which depends only on the three spatial coordinates[25]. The second proves that the energy functional of the electron density follows the variational principle[26], shown in Eq. 2.3.

$$E^{TEST}=\frac{\langle \Psi^{TEST}|H|\Psi^{TEST}\rangle}{\langle \Psi^{TEST}\Psi^{TEST}\rangle}\geq E_0 \qquad \text{Eq. 2.3}$$

It states that the energy evaluated for a general Ψ^{TEST} is always higher than the real energy E_0 of the ground state and $E=E_0$ if and only if $\Psi^{TEST} = \Psi_0$. Thus, the best solution to represent the ground-state is the lowest eigenvalue found as a result of an

optimization problem. Kohn and Sham provided a kay insight to consider a fictitious non-interacting system of electrons, treatment described in the Eq 2.4

$$E[\rho(r)] = -(\frac{1}{2})\sum_i (\int \Psi_i^0(r)\nabla^2\Psi_i(r)dr) - \sum_k \int (\frac{Z_k}{|r-R_k|}\rho(r)dr) + \frac{1}{2}\iint (\frac{\rho(r_1)\rho(r_2)}{r_{12}} d r_1 d r_2)$$

$$+ E_{xc}[\rho(r)] \qquad \text{Eq. 2.4}$$

Where the interaction of the electrons is described by the Electronic-Exchange correlation term $E_{xc}[\rho(r)]$ and the kinetic energy is not described as a functional of the density.

2.1.2 Electronic Exchange-Correlation

The only unknown term in Eq 2.4 is the functional for the description of $E_{xc}[\rho(r)]$, which contains the difference between the interacting and non-interacting systems as well as the non classical electron-electron interactions. Many theories are employed to provide a more accurate description of the electronic correlation and the electronic exchange. The two terms respectively are separable, which means the energy can be expressed as a sum of the Exchange term and the Correlation term. Energy Exchange is described by assuming a uniform electron gas and the following formula is used, as Dirac and Slater did prior to the Kohn-Sham theorems[22].

$$E_x^{UEG}[\rho(r)] = \int \rho(r)\varepsilon_x^{UEG} dr = -(\frac{3}{2})(\frac{3}{4\pi})^{1/3} \int \rho(r)^{(4/3)} dr \qquad \text{Eq. 2.5}$$

Where ε_x is the energy density of a uniform electron gas.

The correlation term is more complex to handle, and the simple approximation of a uniform electron gas in not enough to describe the energy term. The value ε_c is derived by fitting a parameterized function to the result of numerical solutions Schrödinger equation[27–29]. This approach is known as Local Density Approximation (LDA). However, good results are achieved only if the chemical system does not exhibit a wide density variation. To improve this method General Gradient

Approximation[30] (GGA) and *meta*-GGA[31] are widely used. The GGA includes both density and the spatial first derivative of density ε_c in Eq. 2.5. The *meta*-GGA includes both the first and second derivative of the electron density. For this work, a hybrid-*meta*GGA ωB97XD DFT functional[32] was employed, it mixes the short-range and long-range exchange of non-interacting electrons as provided in Hartee-Fock theory with the short-range exchange and correlation energy derived from DFT, in order to minimize the spurious self-interaction error deriving from the one-electron Hamiltonian. The expression of the exchange-correlation functional is the following.

$$E_{xc}^{\omega B97X} = E_x^{LR-HF} + c_x E_x^{SR-HF} + E_x^{SR-B97} + E_c^{B97} \qquad \text{Eq. 2.6}$$

Where c_x is a small fraction number ranging from 0.2-0.25, $E_x^{\text{LR-HF}}$ and $E_x^{\text{SR-HF}}$ are the long-range and short-range exchange terms of Hartree-Fock theory while $E_x^{\text{SR-B97}}$ and E_c^{B97} are the short-range exchange and the correlation energy present in the B97 functional respectively.

2.2 Dispersion Corrections

There are many approaches to take into account the non-covalent interactions as a result of a long range Van Der Waals forces. For the ωB97XD[32] functional the description of this effect is taken into account using the Grimme-D2 dispersion corrections. The correction is made by adding the term E_{disp} to the evaluated DFT energy, shown in the following equation.

$$E_{disp} = -\sum_{XY}\sum_{n=6,8} s_n \frac{C_n^{XY}}{r_{XY}^n} f_{d,n}(r_{XY}) \qquad \text{Eq. 2.7}$$

C_n^{XY} denotes the averaged isotropic *n*th-order dispersion coefficient for an atom pair XY , s_n is the global scaling factor, r_{XY} the distance between the atom pair, and $f_{d,n}$ a dumping function that determine the range of the dispersion correction.

2.3 Basis Set

The basis set is a mathematical representation of the atomic orbitals, and hence of Ψ, using a linear combination of adequate functions. The most reliable representation is given by the Slater Type Orbital (STO). Although its shape is very suitable to describe the atomic orbital, these functions are not easy to manipulate in mathematical treatments since the evaluation of their integral may be challenging. As a solution, Gaussian functions are used[33]. The STO function and the GTO function are respectively shown in Eq. 2.8 and in Eq. 2.9.

$$\gamma(x,y,z,\alpha,i,j,k)=N x^i y^j z^k e^{-\alpha(r)} \qquad \text{Eq 2.8}$$

$$\gamma(x,y,z,\alpha,i,j,k)=N x^i y^j z^k e^{-\alpha(r^2)} \qquad \text{Eq. 2.9}$$

Where N is a normalisation constant; x, y and z represent the Cartesian coordinates for orbital symmetric corrections; α is the amplitude of the function while *i*, *j* and *k* describe the orbital type:

s-type orbitals : $i = j = k = 0$

p-type orbitals : $i + j + k = 1$

d-type orbitals : $i + j + k = 2$

However, this description still lacks accuracy since the center of the Gaussian needs a better description for the close-to-nucleus environment and the tails of the Gaussian drop down really fast compared to the orbital energy trend. Therefore, in order to reach the same shape accuracy of the STOs, as introduced by Pople at *ali*[34], a linear combination of Gaussians is used.

$$\psi=\sum_i^M c_i \gamma(x,y,z,a,i,j,k) \qquad \text{Eq. 2.10}$$

Where c_i is the contraction coefficient chosen to ensure normalization and optimize the shape and γ is the gaussian function. This basis set is known as STO-*n*G, in this nomenclature *n* is the number of Gaussian functions employed. So far, we have

reached an adequate representation of the core orbital system. Valence orbitals are more susceptible to the electron density variation and a more flexible description needs to be carried out. A common approach is to break down the atomic valence orbitals into two base functions, each of them described by a linear combination of Gaussian functions. The nomenclature of such a basis set is N-XYG[35,36]. Where N corresponds to the integer value *n* for the STO-nG for the core orbitals description; the first base function is described with X number of Gaussians and the second base function is described with a Y number of Gaussians. The differences between the X and Y functions are to research in the parameter α of Eq.2.9, with the idea that a combination of "tight" and "wide" Gaussians is able to reach the same flexibility of valence orbitals. To improve molecular description polarisation functions and diffuse function are usually added. Polarization functions include in the basis set a higher angular momentum orbital to improve flexibility of bond description along the three dimensional coordinates *x*, *y* and *z*. This means that a *p*-type orbital is also described with *d*-type orbital and a *d*-type orbital is also described with *f*-type orbitals. To the previous nomenclature N-XYG a "(*d*, *p*)" term is added, where *d* is referred to atoms heavier than He and *p* is referred to H and He atoms. Diffuse functions help describe a system with a high difference of electronic density distribution, for systems that present high electronegative atoms, EWG and for ionic systems, allowing electrons to lie far from the nucleus. For these functions the term "+" is added to the previous nomenclature. The choice of this basis set is founded on the good results obtained in the DFT study of organometallic reaction[23,38]. Ultimately, due to the description of transition metals and heavy atoms, which need to include the relativistic effect of core electrons, a set of analytic functions called Effective Core Potential[39] (ECP) are used.

2.4 Modelling of Solvent Effect

Since the catalyst used for this project were calculated under the effect of solvents in literature, a brief explanation of this approach is provided. Typically, the solvent effect is described with an implicit or explicit method. The explicit method is often

challenging since the solvation shell is built placing the solvent molecules around the solute according to the specific solute-solvent interactions. Therefore, in addition to the computational cost of this procedure is often challenging to find the solvent distribution which faithfully represent the experimental case. Moreover, crucial parameters are the number of solvent molecules used, and an accurate entropy calculation for the correct free energy evaluation is needed. An approximation of this method that provides an acceptable result is the implicit method[40], where the solute is surrounded by a solvent described by a continuous uniform and polarizable medium with dielectric constant ε, employing a Self Consistent Field calculation. In this approach, the charge distribution of the solute and the solvent interact mutually until the convergence is reached. In particular, the $Pd(PPh_3)_2$ catalyst was calculated using *THF* as solvent with a dielectric constant ε = 2.379; the *PEPPSI* catalyst was calculated in *1,4-dioxane* with a dielectric constant ε = 2.25; the *Xantphos* catalyst was calculated using *o-Xylene* as solvent with a dielectric constant ε = 2.57 while the *Grubbs II* was calculated in CH_2Cl_2 with dielectric constant ε = 9.1.

2.5 Molecular Mechanic force fields

The broad spectrum of interactions is the essential building block for chemistry and its rationalization is the main driving force for the development of chemical science. A full description of the organization of electrons among atoms is a complex and multifaceted process and is only possible in the boundaries of quantum mechanics. The density functional theory is a common choice for the ground-state calculations but it becomes unsuitable for extended size systems and long time scale. Therefore, the chemical interactions are often treated with simplified atomistic models called force fields. It consists of an analytical function of the atoms' position, which generally depends on a number of unknown parameters to be determined. They are traditionally employed to investigate a small portion of the potential energy surface based on atomistic models which are inspired by the chemical understanding of the system. In spite of its computational properties, in general, it lacks the necessary flexibility and

accuracy to describe the spectrum of interactions that defines the chemical bonds. For transition metal complexes the description of coordination bonds is particularly challenging due to the nature of force fields. However, in recent years machine learning frameworks witnessed the possibility of a suitable representation of the chemical environments with the combination of ridge regression-base FF with bispectrum functions[41,42]. Thus, in this project, we selected a spectral neighbor analysis potential (SNAP) force field since it is able to account for any fundamental feature of chemical bonds without any assumption on the chemistry of the bonds considered[42].

2.5.1 SNAP Force Field

The general representation of the potential energy surface in terms of quantum mechanical energy can be considered as an energy function that depends on a set of nuclear coordinates $E^{QM}(R_i)$, by means of an FF, $E^{FF}(R_i,a_j)$ with a_j the unknown coefficients to be determined. The parametrization of PES requires two fundamental steps:

- the definition of a feature vector to describe the geometry system
- the definition of the relationship between this vector and the energy of the system

The chemical environment of an atom is described in terms of atomic density ρ.

$$\rho=\sum_i W_{Zi}\delta(r-r_i) \qquad \text{Eq 2.11}$$

Where ρ is the atomic density, *i* runs over the neighbors of the atom within the same cutoff and W_{zi} is a unique weight factor assigned according to the atomic species. The equation 2.11 represent a 3D description of the local atom environment. The so defined density still lacks a numerical representation of the feature vector as well as symmetric properties such as rotational and translational invariance. A solution to this problem has been found in the construction of a series 4D hyper-spherical harmonics[43] $U^j_{m,m'}$ (θ_0 , θ, Φ) for j= 0, ½, 1… and m, m' = -j, j+1, … ,j-1, j. When the rotation is parametrized in terms of Euler angles, thus invariant to rotation and

translation, these functions are known as Wigner functions. We derive the bispectrum below closely following the notation of Ref.[43] The general density is:

$$\rho(r)=\sum_{j=0,1/2,\ldots}^{\infty}\sum_{m=-j}^{j}\sum_{m'=-j}^{j}u^{j}_{m,m'}U^{j}_{m,m'}(\theta_0,\theta,\Phi) \qquad \text{Eq 2.12}$$

where m, j and l are the symbols that define the Wigner matrix and $u^{j}_{m,m'}$ are the expansion coefficients given by the inner product of the neighbor density with the basis function[44]. Since the neighbor density is a weighted sum of δ-functions, each expression coefficient can be written as a sum over discrete values of the corresponding basis function.

$$u^{j}_{m,m'}=U^{j}_{m,m'}(0,0,0)+\sum_{r_{ii'}<R_{cut}}f_c(r_{ii'})w_iU^{j}_{m,m'}(\theta_0,\theta,\Phi) \qquad \text{Eq. 2.13}$$

Where the function f_c is the atom density in the local environment.

The expansion coefficients u^{j} are not directly useful as descriptors, because they are not invariant under rotation of the polar coordinate frame. However, the following scalar triple products of expansion coefficients can be shown to be real-valued and invariant under rotation.

$$B_{j1,j2,j}=\sum_{m_1m_1'=-j_1}^{j_1}\sum_{m_2m_2'=-j_2}^{j_2}\sum_{m,m'=-j}^{j}(u^{m,m'}_{j})H^{jmm'}_{j_1m_1m'_1j_2m_2m'_2}u^{j_1}_{m_1m'_1}u^{j_2}_{m_2m'_2} \qquad \text{Eq. 2.14}$$

Where the constant H are couplings coefficients analogous to the Clebshc-Gordan coefficients for rotations on 2-sphere[41]. These invariants are the components of the bispectrum. They characterize the strength of density correlations at three points on the 3-sphere. The order of the bispetrum component j defines the number of coefficients generated. The lowest-order components describe the coarsest features of the density function, while higher-order components reflect finer detail.

To fulfill the second requirement for the PES parametrization a brief explanation of the relationship between the bispectrum components and the energy evaluation is provided. The energy obtained can be accurately reproduced by linear combinations

from the lowest order set of K bispectrum components, with linear coefficients that depends only on the chemical identity of the central atom.

$$E^{i}_{SNAP}(B^{i}) = \beta^{\alpha_i}_{0} \sum_{k=1}^{K} \beta^{\alpha_i}_{k} B^{i}_{k} = \beta^{\alpha_i}_{0} + \beta^{\alpha_i} B^{i} \qquad \text{Eq. 2.14}$$

Where α_i is the chemical identity of the i atom and $B_k^{\alpha i}$ are the linear coefficients for atoms type α. Hence the problem of generating the interatomic potential has been reduced to that of choosing the best values for the linear SNAP coefficients.

The general assumption of this model is that the energy of the system containing N-atoms can be decomposed into the sum of atomic energies, which in turn can be written as a linear function of their bispectral components.

$$E^{FF}[(R_i),(a_j)] = \sum_{l}^{N_{atom}} E_l[(R_i),(a_j)] = \sum_{l}^{N_{atom}} \sum_{j}^{N_{2j}} a^{l}_{j} B^{l}_{j}(R_i) \qquad \text{Eq 2.15}$$

Where l in the chemical specie, j is the finger print of the n-body atomic environment that define the order of the bispectrum components, a_j are the coefficient to be determined and $B(R_i)$ are the bispectrum components which depends of the sole' Cartesian coordinates. There is no rigorous mathematical proof that the total energy can be written as a sum of atomic energies. However, this formulation provides a high flexibility way to represent the PES, whose accuracy can be validated with the accuracy of the predictions made. As a consequence, a large flexibility degree of flexibility in the FF is required which means that a large number of coefficients are required. The number of the function in series (N_{2j}) can be tuned by increasing their maximum order, 2j. Expanding the chemical environment over a growing number of bispectrum components improves the accuracy of the description.

2.6 Molecular Dynamic simulations

For this project, the Molecular Dynamics simulations are carried out in LAMMPS(ref) (Large-scale Atomic/Molecular Massively Parallel Simulator). The principles of a classical molecular dynamics simulation are quite straightforward. It is based on the

resolution of Newton's equations of motion for a number of atoms. The input provides an initial list of the positions and velocities of the atoms in the system and a description of particle interactions. These interactions determine the forces acting on the atoms and since the masses of the atoms are known, their accelerations can be calculated. The equations governing molecular dynamic simulations are:

$$F_i = -\left(\frac{\partial U}{\partial r_i}\right) \qquad \text{Eq. 2.16}$$

$$a_i = \frac{F_i}{m_i} \qquad \text{Eq. 2.17}$$

Where F_i is the force acting on atom i, U is the total potential energy of the system, r_i is the position of the atom i, a_i is the acceleration of atom i, and m_i is the mass of atom i. As a consequence of the of Newton's law it is possible to calculate the position and the velocity of each atom after a small increment of time. The most widely used algorithm to calculate this variable is the velocity Verlet algorithm[49], usually in the form of a Taylor expansion.

$$r_i(t+\Delta t) = -r_i(t-\Delta t) + 2r_i(t) + \frac{\Delta t^2}{m_i}(F_i(t)) \qquad \text{Eq. 2.18}$$

$$v_i(t) = \left(\frac{1}{2\Delta t}\right)[r_i(t-\Delta t) - r_i(t-\Delta t)] \qquad \text{Eq. 2.19}$$

With this scheme, the error associated with the position and the velocity are respectively of the order of Δt^4 and Δt^3. The value Δt is defined as timestep. The choice of this parameter is important since it should be small enough to guarantee an acceptable error in terms of evaluation of velocity and position. Another fundamental feature is the definition of the thermodynamic properties such as the kinetic energy, the temperature and the pressure of the system. The kinetic energy evaluation and the temperature are strictly correlated since both depend on the evaluation of the average velocities of all the atoms.

$$K = \sum_{i=1}^{N} 1/2\left(m_i v_i^2\right) \qquad \text{Eq. 2.20}$$

Where K is the total kinetic energy, N is the number of atoms of the system, m is the mass of the i atom and v is the velocity of i atom. While the calculation of the temperature arises from the following formula.

$$K=(3/2)k_B T \qquad \text{Eq. 2.21}$$

Where k_B is the Boltzmann constant and T is the temperature of the system.

At last, the pressure P of the system can be computed at each time step with the following expression.

$$P=\frac{N k_B T}{V}+\frac{\sum_{i=1}^{N} r_i F_i}{3V} \qquad \text{Eq. 2.22}$$

Where V is the volume of the system.

In LAMMPS the volume where the atoms are contained is called the simulation box, it has the shape of a cube defined by three dimensional edges (x, y and z). An important feature related to the definition of the simulation box is the boundary conditions. This allows defining what happens when an atom reaches the edges or exceeds them. To minimize the effect of the box a common approach is to use periodic boundary conditions, in this way the simulation box is surrounded by 26 identical replicas of itself and at each timestep the total force F_i acting on each atom is computed only for the ones inside the simulation box, while the atoms contained in the other boxes are totally neglected in the calculation.

Since the main purpose of this project is to use the Molecular Dynamics simulations to test the SNAP force field fitted and to perform an automated conformational search is important to define in which ensemble the simulations were carried out. So far the MD algorithm considered the total energy of the system is constant over time because there no external parameter was taken into account. Thus the system we are analyzing can be considered an isolated system. According to the MD each atom of the system is under the effect of a conservative force, therefore its mechanical energy is to be considered constant. A system where the number of atoms N, the total energy E and

the volume V are constant is called a microcanonical ensemble (NVE). The assumptions behind the definition of this system cannot reproduce many experimental data since usually they are obtained under conditions of constant temperature and pressure. In particular, for our calculation, we selected a canonical ensemble (NVT) where the number of atoms, the temperature and the volume of the system are constant.

2.7 Clustering Analysis

To improve the parametrization of the SNAP force field is important to provide an adequate representation of the degrees of freedom of each catalyst. Therefore, is important to provide a tool that is able to generate a consistent amount of conformational isomers exploring the interested conformational space. This usually leads to rough data containing a sampling of very similar structure, thus, in order to refine the data set and avoid redundant informations, a Cluster analysis is needed. It is based on a method that locates clusters of geometrically similar conformers in ensembles of chemical conformations. The general algorithm defines a pairwise inter-conformational distant matrix in either torsional or Cartesian space defining a hierarchy of clusterings[45] into a set of conformationally related subfamilies. For this project, the criterion followed for the cluster analysis is based on the definition of the Kelley Penalty function[46]. The first stage of the algorithm calculates the distant matrix *NxN* superimposing all the conformers together and according to a specific cutoff the first clusters are generated. Subsequently, the distance between two clusters *m* and *n* is then calculated with the following equation.

$$Dist(m,n)=\frac{(\sum_{i=1}^{X}\sum_{j=1}^{Y} dist(i,j))}{XY} \qquad \text{Eq. 2.23}$$

Where the cluster *m* contains X members and the cluster *n* contains Y members and the *dist(i,j)* term is the root mean square (RMS) distance between the two members, *i* and *j,* of clusters *m* and *n* respectively, after the superimposition. At each stage of the

clustering algorithm a search is performed and the two nearest clusters are merged together and the spread of each cluster is calculated. The spread of a cluster *m* containing N members is given by:

$$spread_m = \frac{\left(\sum_{k=1}^{N} \sum_{i=1, i<k}^{N} dist(i,k)\right)}{\left(N(N-1/2)\right)} \qquad \text{Eq. 2.24}$$

Where *i* and *k* are members of cluster *m*.

The average spread is then given by the following equation.

$$AvSp_i = \frac{\sum_{m=1}^{cnum_i} spread_m}{cnum_i} \qquad \text{Eq. 2.25}$$

where $cnum_i$ is the number of clusters at the stage *i* of the clustering.

Once the clustering is complete, the set of $AvSp_i$ values is normalized to lie within the range 1 to *N*-1, with *N* the number of structures in the original data set according to the following equation:

$$AvSp(norm) = \frac{N-2}{Max(AvSp) - Min(AvSp)}\left(AvSp_i - Min(AvSp)\right) + 1 \qquad \text{Eq. 2.26}$$

where *Max(AvSp)* and *Min(AvSp)* are the maximum and the minimum values respectively of average spread. At end of the each stage of clustering *i*, a penalty value P_i is calculated on the base of the total number of clusters at step *i,* $nclus_i$.

$$P_i = AvSp(norm)_i + nclus_i \qquad \text{Eq. 2.27}$$

At the end of the process, it is possible to identify the number of clusters that exhibit the lowest Kelley Penalty value. It defines the state where the clusters are as highly populated as possible while maintaining the smallest spread. For each cluster is then provided a single conformer that represents the centroid of the cluster.

2.8 Computational Details

The DFT energies obtained in this project were calculated employing the dispersion-corrected hybrid exchange correlation DFT functional ωB97XD[32], as implemented in the Gaussian09 software (Revision A.02)[50]. Pd, Ru, Br atoms are described using Lanl2dz effective core potentials (ECP) and their corresponding double-zeta basis set with an additional *d*, *p*-polarization function for Br (respectively exponent 0.428 and 0.0376), *f*-polarisation function for Pd (exponent 1.472) and Ru (exponent 1.235)[47]. C, H, P, O, Si, Cl and N atoms were described using a double-zeta 6-31G(d,p). Cl, O and N atoms were also described with a diffuse function 6-31+g(d).

The geometry optimization has been carried in vacuum without imposing any symmetry constrains. TS geometries were relaxed along the reaction coordinate to verify the connection with the expected reactant and product. At last, a vibration calculation has been performed for each TS and reaction intermediate in order to verify the presence of only one imaginary frequency and all real frequencies respectively

The conformational search was carried out with Macromodel as provided by Schrödinger Maestro software. The parameters selected for the conformational search are provided in four different panels. (I) In the potential panel we selected OPLS3e[52] as the only available force field for the conformational search with dielectric constant ε =1. The cutoff adopted is the "normal" which includes a Van deer Waals cutoff of 7.0 Å, the electrostatic cutoff of 12.0 Å and the hydrogen bond cutoff of 4.0 Å. (ii) In the Csearch panel, we selected a Monte-Carlo multiple minima approach (MCMM)[51] assigning to each torsion a rotation value between 0-360° with a number of steps equal to 6000. The maximum atom deviation parameter was set on a value of 0.5 Å and the window energy was set of a value of 200 Kj for all the catalyst with the exception of the Xantphos, with a window energy of 300 Kj. (iii) In the minimization panel we selected the Polak-Ribier Conjugated Method (PRCG) with a number of 2500 iterations with the convergence on movements with a threshold of 0.05 Å. (iv) In the constrains panel we constrained all the coordinates of the reagents and bonds of the metal core for each catalyst.

The fitting and the refinement of the SNAP force field potentials were done through the Fortran code fitsnap. Such a code uses large-scale atomic/molecular massively parallel simulator (LAMMPS) as an external library to generate the bispectrum components for all atoms and to accordingly calculate molecular dynamics runs. In all cases, the order of 2j=8 for the bispectrum components, corresponding to 56 coefficients for each atomic kind, was used. The regularization parameter λ for the fitting was set on the value of 1.0. The radial cutoff for each atomic kind was set on the value of 4.1, with the exception of the hydrogen which was reduced by a factor of 0.6. The weight of each atomic kind in the refinement of the coefficient of each bispectrum component was set to unity.

The MD simulations were all carried out constraining the reaction coordinate and all the bonds of the transition metal complex in a simulation box with periodic boundary conditions. The minimization was carried out at 0 *K* with a 0 input of velocity for each atom for a number of 1000 steps and timestep set to 10. The MD trajectories were run at 100K, 300K and 400K for the $Pd(PPh_3)_2$ for a number of 50000 steps with a timestep of 0.5. The velocity input was randomly generated from a Gaussian distribution for all the atoms.

Chapter 3. MACHINE LEARNING APPROACH

First, we will give a general explanation of the Machine Learning approach and then we will explain the specific methodology we applied for this project. The first step of the Machine Learning approach is the choice of a model that consists of a mathematical equation that contains a *N*-number of coefficients to be determined. The second step consists in the generation of the training set, a list of data that contains all the information necessary for the model to be trained. The training is carried out fitting the parameter selected in the model refining the coefficients, usually through regression methods. At last, the optimized model is employed for prediction of a specific property benchmarking the model on a test set. The test set is made up of a

similar sampling of the training set but composed of data never trained by the force field. If the final results are satisfying the training of the model stops. If the results are not satisfying the training set can be enlarged and the model selected is optimized to lower the error on the predictions. Here is provided a general scheme of a machine learning approach.

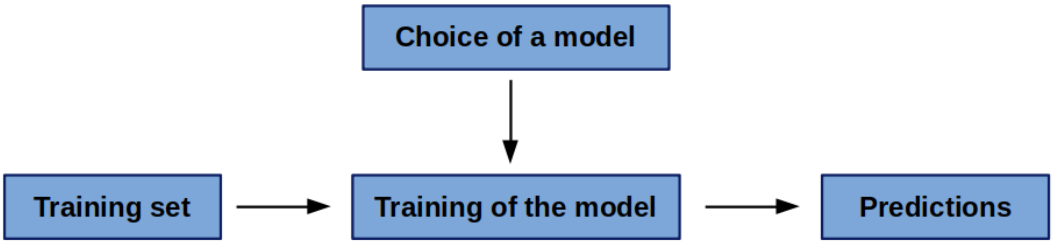

Figure 3.1.- *Machine Learning canonical approach.*

3.1 Fitting Strategy

In our case the general approach can be summarized in the scheme below.

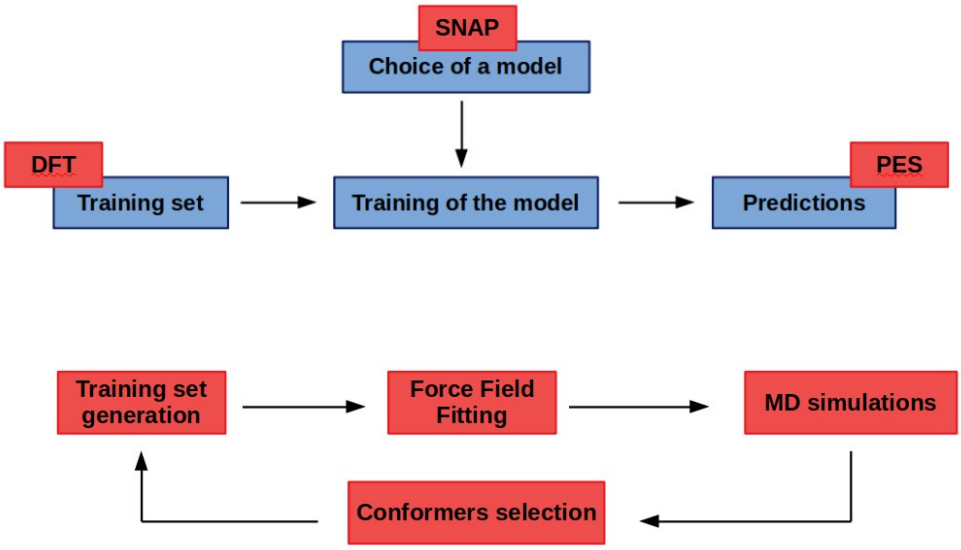

Figure-3.2. *Selected Machine Learning approach.*

The model we decided to select for the ML is the SNAP, due to the good results in the PES parametrization reported in literature[42] as discussed in the theoretical principles section. A crucial aspect of the ML is the generation of the training set. It is composed of the conformers' geometries with the the relative DFT energies obtained through a Single Point calculation. The geometries are generated by a conformational analysis performed with Macromodel , as provided by the demo version of Schrödinger Maestro. Subsequently, to refine the data set, a clustering analysis is performed. In this way, the number of the conformers is reduced and the elimination of redundant informations results in a higher quality data set. To include informations about stretching and bending a random atom displacement is applied for each atom of each catalyst. Refined the number of the structure we then proceed with the fitting of the force field. The determination of the unknown coefficient has been carried out with the use of a ridge regression that minimizes the difference between the QM energies and the force field's predictions, expressed in Eq 3.1.

$$Min(a_l)=[||E_0^{QM}(R_i)-E^{FF}(R_i,a_l)||^2+\lambda||a_l||^2] \qquad \text{Eq. 3.1}$$

Where the constant λ is the regularization parameter, E_0^{QM} are the energies calculated with the single points at a DFT level theory and E^{FF} are the energies predicted on the base of the fitted coefficients α . The introduction of a regularization parameter has the effect of selecting the smoothest solution among the many quasi-degenerate solutions of the simple linear least-square problem. This becomes crucial when the number of parameters to be determined is larger compared to the number of QM reference energy values.

When the fitting process is complete the QM energies and the predicted energies of the conformers employed in the training set are listed in output file where the root mean square of the fitting is reported. For the fitting, the order of the bispectrum components is set on the value of 2j=8 which results in a number of 56 coefficients to be determined for each atomic kind. Good fitting results in a low root mean square deviation of the energy of the training set compared to the total energy window of the training set, meaning that the number of coefficients selected are flexible enough to

allow a correct parameterization. To test the stability of the force field generated a molecular dynamic simulation is performed. It consists of two main steps. With a temperature set on 0 *K*, a minimization is carried out in vacuum to verify the knowledge of the force field in the description of a conformational space close to the transition state. Subsequently, at the temperature of 100K, 300K and 400K an MD trajectory is run to verify the stability of the force field for the activated movements of stretching and bending and torsions of the interested degrees of freedom investigated in the conformational analysis. During the benchmark, we must ensure that thermal fluctuations will not bring the system in a region of the phase space totally unexplored by the training set. If the force field stability is not confirmed by the result of the MD, an enforced training set is required to optimize the parameters of the conformational search until the parametrization gives a stable molecular dynamic trajectory. If the stability of the force field is confirmed by the MD trajectories an active learning procedure is implemented. It consists in the run of long MD trajectories at a temperature where all the atomic movements are allowed. A number of configurations are extracted from the trajectory and using the Gaussian metric of the Eq. 3.2 we can define if they are distant enough to be included in the training set itself and fitted.

$$d(\|B^l(R_i)-B^l(R_j)\|)=\exp\left(-\sum_v (B^l_v(R_i)-B^l_v(R_j))^2/2\sigma_l^2\right) \qquad \text{Eq. 3.2}$$

Where d is the distant metric, $B^l(R_{i,j})$ are the bispectrum components of the l atomic kind that differs in R_i and R_j Cartesian coordinates, v is the number of the bispectrum components and σ_l is a hyperparameter that sets the procedure selectivity. If the bispectrum components' distance is higher than an arbitrary value the relative conformers are then included in the training set.

The newly enlarged system is then employed for a new MD trajectory in an iterative cycle. Once the error of the training set is sufficiently narrow and the conformational space is explored on a wide space phase, a thermal annealing is performed to find the global minimum of the PES obtained. The conformers found are then optimized to TS and relaxed along their reaction coordinate to confirm the formation of expected reagents and products. Subsequently, a single point calculation is performed with the

solvent effect corrections in order to compare the result obtained with the experimental data and verify the identification of a lower transition state.

Chapter 4. RESULTS AND DISCUSSION

4.1 Transition States Optimization

First of all, the transition states were optimized with the DFT functional and the basis set discussed in the computational details section and the resulting geometries are compared with the reference values present in the literature. For each catalyst we here compare first the reaction coordinate and the chemical bonds that define the environment of the transition metal core.

- ***$Pd(PPh_3)_2$***

The reaction coordinate selected for the TS optimization is the cleavage of the Br-C bond. The transition state identified confirms that the reaction occurs with a concerted mechanism involving the breaking of the σ bond between the bromine and the aryl group and the simultaneous formation of two σ bonds, the first between the palladium and the bromine and the second between the palladium and the carbon of the aryl group.

Bond	***Reference value (Å)***	***Optimized (Å)***
C-Br	2.26	2.21
Pd-Br	2.61	2.61
C-Pd	2.13	2.12

Table 4.1-*Bond length comparison between theoretical reference values and the optimized values of $Pd(PPh_3)_2$ catalyst TS. In red the reaction coordinate.*

As shown in table 4.1 the bond length of the reaction coordinate C-Br and the bond length of the Pd-Br and C-Pd are in good agreement with the theoretical values. The transition state was relaxed along its reaction coordinate confirming the connection with the expected reagent and product.

- ***PEPPSI***

The transition state was optimized along the coordinate N-Ar, the sigma bond formed which allows the reductive elimination to occurs. It is characterized by the formation of a triangular transition state at the vertex of which are present the palladium atom, the nitrogen atom of the aniline and the carbon atom of the phenyl compound. The reaction mechanism confirms that the cleavage of the Pd-Ar bond happens simultaneously to the formation of the new N-Ar bond resulting in the formation of a diphenylamine molecule where the nitrogen is still coordinated to the metal complex with a bond length of 2.23 Å.

Bond	***Reference value (Å)***	***Optimized (Å)***
Pd-N	2.05	2.02
Pd-Ar	2.10	2.05
N-Ar	1.95	1.94

Table 4.2*- Bond length comparison between theoretical reference values and optimized values of PEPPSI catalyst TS, in red the reaction coordinate.*

As shown in table 4.2 the bond length of the reaction coordinate and the bond lengths of Pd-N and Pd-Ar are in good agreement with the theoretical data. The transition state was relaxed along its reaction coordinate confirming the connection with the expected reagent and product.

- ***Grubbs II***

The transition state was optimized along the cleavage of the H_2C-CSi bond. The optimized transition state confirms the reaction mechanism of the reversible [2+2] cycloaddition with the formation of the ruthenium complex coordinated to the trichloridesilidene and the styrene.

Bond	***Reference value (Å)***	***Optimized (Å)***
Ru-CPh	2.18	2.18
Ru-CSi	1.81	1.86
PhC-CH2	1.41	1.41
H_2C-CSi	2.27	2.20

Table 4.3.- *Bond length comparison between theoretical reference values and optimized values of Grubbs II catalyst TS, in red the reaction coordinates.*

As shown in table 4.3 all the bonds selected near the environment of the reaction coordinates show a good agreement with the literature references. The transition state was relaxed along the reaction coordinates confirming the formation of the expected reagent and product.

- ***Xantphos***

The transition state was optimized along the reaction coordinate which involves the cleavage of the O-H bond. A negative frequency confirmed the identification of the transition state and the relaxation along the reaction coordinate confirmed the formation of the expected reagent and product. This confirms that the mechanism of the reaction consists in the cleavage of the O-H bond and the simultaneous formation of a new bond between the ruthenium and the hydrogen.

Bond	*Reference value (Å)*	*Optimized (Å)*
Ru-O	2.23	2.22
Ru-H	1.68	1.67
O-H	1.40	1.37

Table-4.4 *Bond length comparison between theoretical reference values and optimized values for Xantphos catalyst TS.*

As shown in table 4.4 the bond length of the reaction coordinate and the bond lengths of the metal complex with the oxygen atom and the hydrogen atom are in good agreement with the literature references.

The general conclusion is that all the catalysts were correctly optimized in their relative transition states confirming for each of them the correct identification of the reaction coordinate since all the relaxation along the reaction coordinates confirmed the formation of the expected reagents and products.

The results of the optimization in terms of free energy activation barrier are reported in the following table.

Catalyst	*ΔG^{+} optimized (Kcal/mol)*
$Pd(PPh_3)_2$	13.7
PEPPSI	19.0
Grubbs II	10.9
Xantphos	22.3

Table-4.5 *Free Gibbs Energy comparison between theoretical data and optimized transition states.*

The activation barrier, as reported in table 4.5, are in agreement with the reactions mechanisms since they all represent reversible reactions we expect to have relatively low activation barriers.

4.2 Conformational Search

A crucial aspect to provide an optimum parameterization of the force field is the representation of all the information the force field requires to run a stable MD. Thus we must provide in the MD input a number of conformers which allows the description of the conformers very different in energy and geometry from the starting transition state. To fulfil this purpose a conformational analysis is carried out through the use of the demo of macromodel software as provided by Schrödinger Maestro.The starting conformational search is a process that consists of two separate parts, the first aims to generate a sampling of conformers differentiated from the value of the torsions angle of the ligands and the ligand's substituents; the second aims to generate a sampling of conformers differentiated from short displacements of every atom of the catalyst, in order to enhance the knowledge of stretching and bending of the force field.

4.2.1 Torsional Sampling

Since the analysis aims to identify only the conformers of the transition state, all the coordinates of the reactants and any ligand involved in the reaction coordinate were constrained. Differently, on the rest of the ligands no constrains were applied.

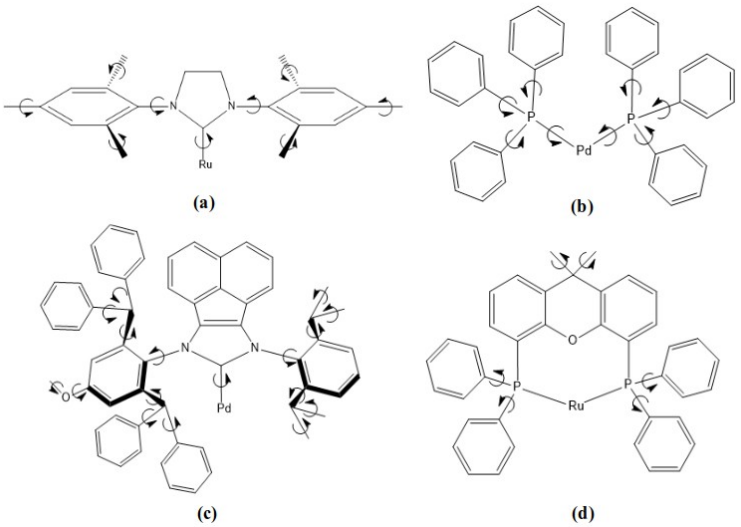

Figure-4.1. *Torsional sampling selection of (a) Grubbs II, (b) $Pd(PPh_3)_2$, (c) PEPPSI and (d) Xantphos.*

A brief summarized table for each parameter of the torsional sampling

Catalyst	***PRCG Convergence***	***Threshold***	***Window energy (KJ)***	***Conformers generated***
$Pd(PPh_3)_2$	Movement	0.05	200	6000
PEPPSI	Movement	0.05	200	5393
Grubbs II	Movement	0.05	200	5968
Xantphos	Movement	0.08	300	5924

Table-4.6. *Parameters for the Conformational search*

The conformational analysis produced a high number of conformers. To validate the quality of obtained conformers a clustering analysis is required.

4.2.2 Clustering Analysis

An important aspect related to the MM-FF fitting is the elimination of redundant informations, thus to refine the initial data population we performed a clustering analysis. It allows to collect a wide data population in smaller populated groups called clusters. The criterion followed to perform the clustering is the Kelley Penalty function to find the state with the highest populated clusters but keeping the spread at the minimum value at the same time.

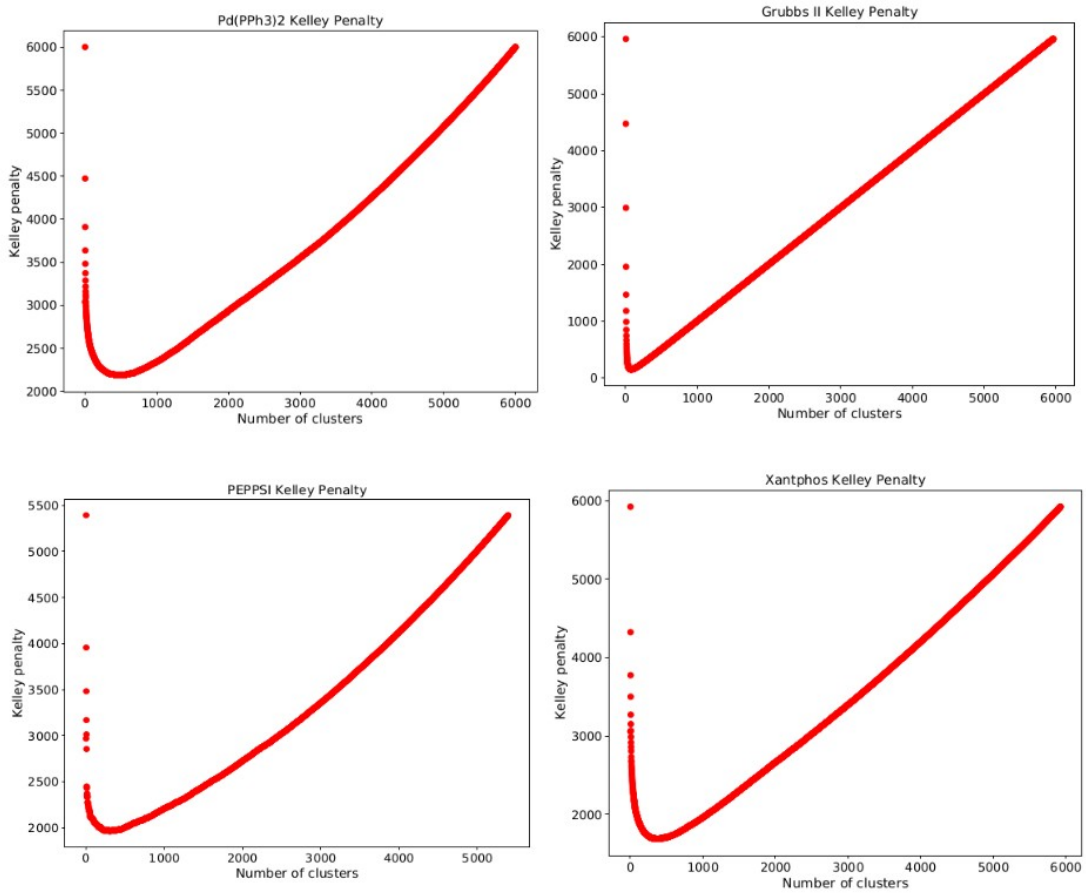

Figure-4.2. *Kelley Penalty function for the cluster analysis of the four catalyst.*

	Number of Clusters
$Pd(PPh_3)_2$	514
PEPPSI	304
Grubbs II	76
Xantphos	369

Table-4.7 *Number of clusters with the minimum Kelley Penalty value.*

The clustering analysis has produced, starting from a sampling of almost 6000 conformers each, a highly reduced number of clusters. The results in table 4.7 are in agreement with the number of the degrees of freedom and the flexibility of each catalyst. As expected the most flexible catalyst, the $Pd(PPh_3)_2$ was reduced to 514

from the starting pull of 6000 conformers. This can be addressed to the wide portion of conformational space explored by the conformational search and due to the fact that the torsions explored does not exceed the window energy selected of 200 Kj. Unlike the latter, the *PEPPSI* catalyst has a very rigid structure represented by the N-heterocycle and a high number of bulky substituents. Therefore, even short torsion results in high energy conformers which are quite above the energy window selected. The combination of the high number of degrees of freedom are in agreement with the final number of cluster found. For the *Grubbs II* the cluster analysis only found 76 different clusters, this result is in line with the low number of significant degrees of freedom, respectively the torsion of the N-heterocycle and its two substituent. In terms of energy, the torsions of the methyl groups are less significant. In addition, the degrees of freedom of this catalyst are not flexible enough to rotate in a range between 0-360° due to the presence the silane structure which minimize the allowed movements. In order to allow a total torsion of the phenyl substituent of the Xantphos we selected a larger energy window, with a higher displacement for threshold to include different conformers in the final output file. As expected the number of conformers are in line with the torsion flexibility of the phenyl groups, in spite of the only four degrees of freedom.

- *$Pd(PPh_3)_2$*

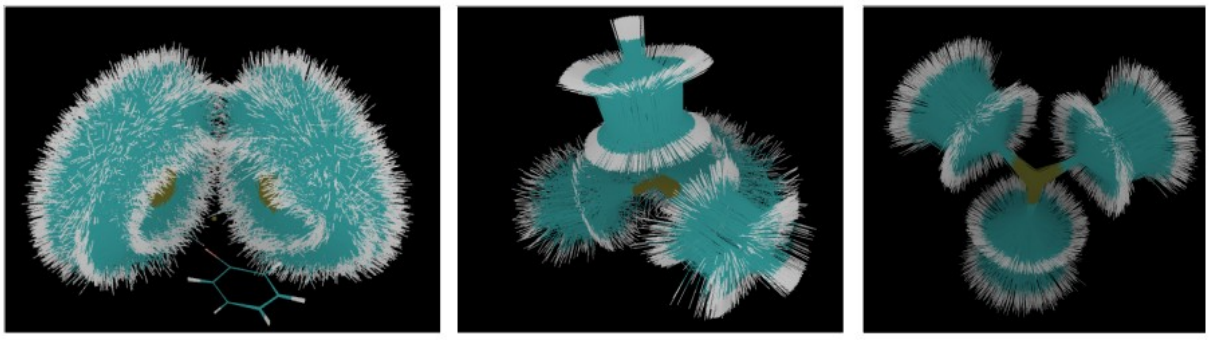

Figure-4.3. *Conformational superimposition of all the clusters of $Pd(PPh_3)_2$ catalyst. (a) Superimposition along the reagents coordinates.(b) Superimposition along P-Ph bond. (c) Superimposition along P-$(Ph)_3$ bonds.*

The figure 11-(a) corresponds to the superimposition of the 514 clusters generated. To clarify the analysis of the torsions analyzed we separate the degrees of freedom in two terms: the torsions around the P-Ph (b) and the torsion of each phenyl substituent (c). For a further simplification, we include the torsional sampling of only one ligand since the final result has shown a certain symmetry between the conformational search of the two ligands. It is possible to see how the parameters selected for the conformational search generated a satisfying sampling along the torsions of all the Ph groups (c), exploring rotations of 360°, and along the torsion of the Pd-P as a consequence of the superimposition (b).

- *PEPPSI*

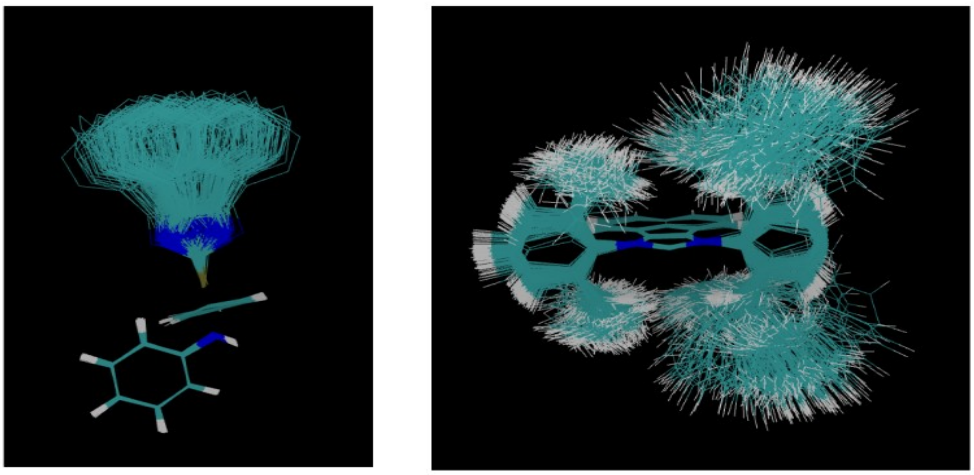

Figure-4.4. *Conformational superimposition of cluster families of PEPPSI catalyst.*

(d)Superimposition along the reagent.(e)Superimposition along the rigid skeleton of the catalyst.

For the PEPPSI catalyst we decided to show the cluster differentiated on the superimposition of two main structures since the total superimposition on the rigid skeleton of the molecule result too complex to be understood. First, we superimposed all the coordinates of the reagents from the cluster analysis, and to simplify the

visualization, we neglected the bulky substituents of the rigid skeleton with the purpose to show the torsion around the Pd-C bond. As it is possible to see from picture (d) a total sampling of 360° has been done for this torsion. To highlight the conformational analysis of the other substituents, we represented a superimposed configuration on the atoms of the rigid skeleton of the molecule and, to simplify the visualization, we neglected the reactants. As it is possible to see from figure (e) all the torsions selected were investigated. Due to the value of the window energy selected for this catalyst, 200Kj, not all the torsions were sampled for a 360° rotation. We can address the reason to the presence of the reactants and a further torsion would result in a conformer with an energy higher than the interval selected.

- *Grubbs II*

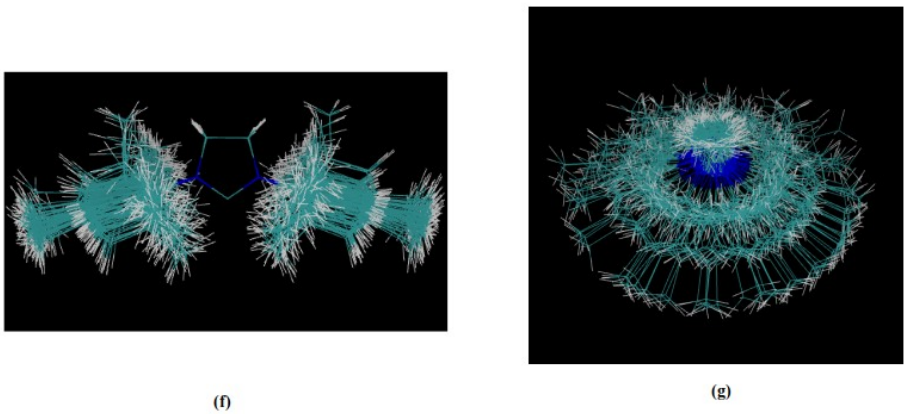

Figure-4.5.*Conformational Superimposition of all the clusters of Grubbs II catalyst. (f)Superimposition on the rigid skeleton of the catalyst. (g) Superimposition on the reactants' coordinates.*

As for the PEPPSI, the total superimposition of the conformers leads to a representation that is hard to understand, for this reason, we decided to superimpose the structures in two different ways. To highlight the torsions of the two substituents of the rigid skeleton of the molecule we superimposed the conformers on the N-heterocycle (f). To represent the torsion along the Ru-C we superimposed the conformers on the reactants (g). For both representations, reactants were neglected. As it is possible to see the torsional sampling was successful, resulting in a 360° rotation

along the Ru-C bond and an almost total rotation of the two substituents of the heterocycle. Again, the non-complete torsions of these two substituents are addressed to the high energy value calculated by the FF in the conformational analysis.

- *Xantphos*

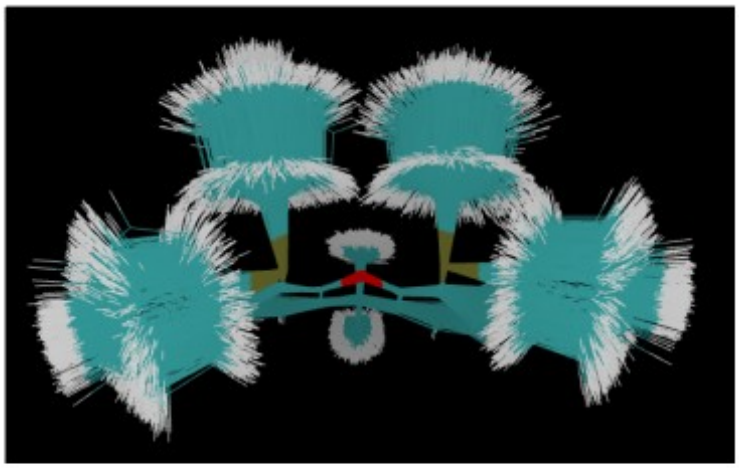

Figure-4.6. *Conformational superimposition of cluster families of Xantphos catalyst.*

Unlike the previous catalysts the representation of the Xantphos's superimposition is quite straightforward, and it is made on the rigid skeleton of the molecule. As it is possible to see from figure 4.6, all the phenyl groups were successfully rotated by 360°. For simplicity, the reactants and the CO were neglected from the representation.

4.2.3 Bending and stretching sampling

The second part of the conformational analysis aimed to include stretching and bending for a better description of the molecular movements in the following MD simulations. All the previous structures were collected in a single file and with a bash script random displacements of every atom of each structures were applied. For each

conformer of the cluster analysis 20 distorted conformers were made, increasing the number of the total conformers of the sampling pull.

	Number of conformers
$Pd(PPh_3)_2$	10280
PEPPSI	6080
Grubbs II	1520
Xantphos	7380

Table-4.8. *Total number of conformers provided for the parametrization*

4.3 Molecular Mechanic Force Field Parametrization

As a model for all the other catalysts in terms of intermediate flexibility and number of degrees of freedom, the $Pd(PPh_3)_2$ was selected to optimize the number of distortions needed for the fitting, refining the total number of conformers needed. The starting conformational sampling was divided into two sets. The training set and the test set. The first aims to parametrize the coefficient and fit the force field each time with a different number of distortions. These set of parameters are then used to evaluate the error associated with the predictions of the energy of the test set. The starting training set consists in the 514 conformers generated with the clustering analysis and only one distortion for each conformer. The other training sets were formed adding each time 3 distortions more for each conformer up to a total number of 16 distortions added for the last training set. The test set consists of the remaining 4 distortions for each conformer previously calculated. The learning curve of this process is here reported.

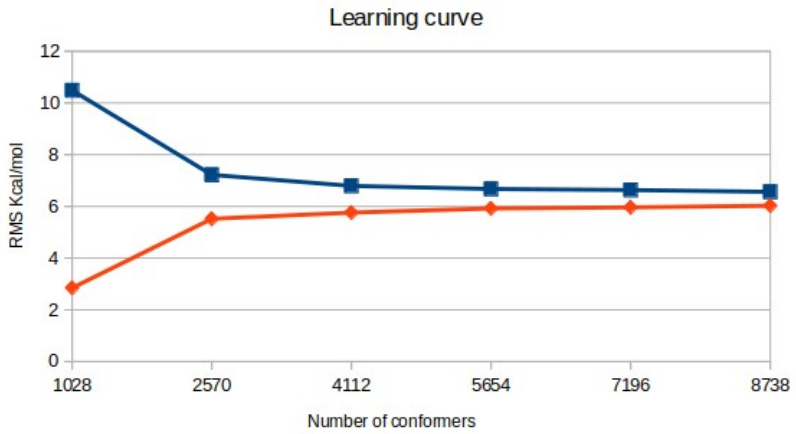

Figure-4.7. *Learning curve of distortions number. The blue line represent the test set, the red line represent the training set.*

In figure 4.7 the *x*-axis represents the total number of conformers (514) and distortions selected for each training set (514*N_{Dist}). The *y*-axis represents the error associated with the the fitting in terms of root mean square deviation. The trend of the learning curve follows the canonical principle of the fitting. By increasing the number of the conformers in the training set the error evaluation increases, while the error associated with the test set decreases, meaning that the accuracy reached for the predictions of the energy increases. The trend errors, as expected, goes to convergence. The final consideration is that after the addition of 10 distortion per conformer the percentage of the error difference is less than 5%, because of this, we decided to proceed with 10 distortions for each catalyst for the parametrization of the bispectrum components with the assumption that the error evaluation is totally addressed to the number of the distortions included. The list of the optimized coefficients for each catalysts are reported in the appendix section.

4.4 Molecular Dynamic Simulations

To test the force field obtained through the parametrization we decided to run an MD simulation that consists of two steps. First, we optimized the geometry with a minimization procedure using the SNAP force field to verify its stability. After the optimization, a random input of velocities was generated and, for each catalyst and a

long trajectory simulation was performed to verify the stability of the force field in the exploration in the surrounding conformational space. The full list of details is available in the computational detail section. For all the MD simulations the reaction coordinates were frozen and all the bonds of the transition metal were constrained.

The result of the Molecular Dynamics simulation has been unsuccessful for the PEPPSI, Grubbs II and Xantphos catalysts. For each of them the geometry optimization procedure resulted in structures with several cleaved bonds. In particular, for the PEPPSI and the Xantphos, the conformers with the highest number of atoms and rigid structure, the optimization resulted in the cleavage of almost all the hydrogen atoms and heavily bent phenyl groups. The Grubbs II simulation resulted in the cleavage of the Silane reagent while the description of the rigid structure of the catalyst and the substituent that were analyzed with the conformational search remained intact during the minimization. As a final conclusion, the parametrization for each of these three catalyst must be optimized.

The Molecular Dynamic simulation of the $Pd(PPh_3)_2$ resulted in a correct minimized geometry and the MD trajectory resulted in a stable simulation. Due to unforeseen events related to the Covid pandemic and the short time available, we decided to proceed only with the $Pd(PPh_3)_2$ catalyst in further MD simulation to test the stability of the force field with higher temperatures. In addition, an MD simulation at 300 K with the same parameters has been run, surprisingly resulting in a stable trajectory. At the end we decided to test if the MD would have been stable at 400K, where all the degrees of freedom are thermodynamically activated. Unfortunately, this resulted in a not stable trajectory. Since the time available was insufficient for the implementation of the active learning no further results are presented.

Chapter 5.CONCLUSIONS AND FUTURE WORK

The results of the optimizations validate the functional and the basis set used resulting in optimized geometries in line with the experimental data. The cluster analysis confirmed that the conformational search carried out with macromodel explored a sufficiently wide conformational space for the interested degrees of freedom for all the catalysts, in agreement with the parameters selected for each conformational search and the relative flexibility of each catalyst. In addition, the cluster analysis turned out to be a powerful tool for the refinement of the data of the conformational search allowing to reduce the fitting computational time. The results of the conformational analysis in combination with the parametrization to generate a training set are considered successful for the $Pd(PPh_3)_2$ catalyst, while not for the others. This suggests an optimization of the parameters selected for the conformational analysis to enhance the clustering analysis and provide a more solid data set for the training. Due to the result of the fitting, we also propose to optimize the order of the bispectrum components 2J including the possibility that 56 coefficients for each atomic kind is not enough to describe the very complex environments for PEPPSI and Xantphos catalysts. In particular, a higher number of bispectrum components leads to a more flexible description of the local atomic environment with the result of a stable MD to implement the active learning procedure. The implementation of the latter is then the natural continuation of the project proposed. Beside, the methodology can be extended considering also other catalysts as promising candidates or the use of a different force field to perform a PES parametrization.

References

[1] Besora, M., Braga, A. A. C., Ujaque, G., Maseras, F. & Lledós, A. *Theor. Chem. Acc.* **128**, 639–646 (2011).

[2] Balcells, D. *et al. Faraday Discuss.* **124**, 429–441 (2003).

[3] Norrby, P. O. & Brandt, P. *Coord. Chem. Rev.* **212**, 79–109 (2001).

[4] Zeini Jahromi, E. & Gailer, J. Probing bioinorganic chemistry processes in the bloodstream to gain new insights into the origin of human diseases. *Dalt. Trans.* **39**, 329–336 (2010).

[5] Hartwig, J. F. *Nature* **455**, 314–322 (2008).

[6] Xue, L. & Lin, Z. *Chem. Soc. Rev.* **39**, 1692–1705 (2010).

[7] McMullin, C. L., Jover, J., Harvey, J. N. & Fey, N. . *Dalt. Trans.* **39**, 10833–10836 (2010).

[8] Hadei, N., Kantchev, E. A. B., O'Brien, C. J. & Organ, M. G. *Org. Lett.* **7**, 3805–3807 (2005).

[9] Lan, X. B. *et al. J. Org. Chem.* **82**, 2914–2925 (2017).

[10] Grubbs, R. H. & Trnka, T. M. *Ruthenium Org. Synth.* 153–177 (2005).

[11] Engle, K. M. *et al. . J. Am. Chem. Soc.* **137**, 5782–5792 (2015).

[12] Luo, S. X. *et al. ACS Catal.* **8**, 4600–4611 (2018).

[13] Śliwa, P. *et al. Organometallics* **35**, 621–628 (2016).

[14] Ledger, A. E. W. *et al*. *J. Chem. Soc. Dalt. Trans.* 716–722 (2009)

[15] Slatford, P. A., Whittlesey, M. K. & Williams, J. M. J. *Tetrahedron Lett.* **47**, 6787–6789 (2006).

[16] Anand, N., Owston, N. A., Parker, A. J., Slatford, P. A. & Williams, J. M. J. *Tetrahedron Lett.* **48**, 7761–7763 (2007).

[17] Blacker, A. J. *et al*. *Org. Lett.* **11**, 2039–2042 (2009).

[18] Takahashi, K., Yamashita, M., Tanaka, Y. & Nozaki, K. *Angew. Chemie - Int. Ed.* **51**, 4383–4387 (2012).

[19] Yu, D. G., Li, B. J. & Shi, Z. J. *Acc. Chem. Res.* **43**, 1486–1495 (2010).

[20] Chmely, S. C. *et al*. *ACS Catal.* **3**, 963–974 (2013).

[21] Born, M. & Oppenheimer, R. *Ann. Phys.* **389**, 457–484 (1927).

[22] Dirac, P. A. M. *Math. Proc. Cambridge Philos. Soc.* **26**, 376–385 (1930).

[23] Slater, J. C. *Phys. Rev.* **81**, 385–390 (1951).

[24] Thomas, L. H. *Math. Proc. Cambridge Philos. Soc.* **23**, 542–548 (1927).

[25] Chu, C. H. & Leung, C. W. *Integr. Equations Oper. Theory* **40**, 391–402 (2001).

[26] Jung, J. Y. *et al. . Korean J. Physiol. Pharmacol.* **10**, 289–295 (2006).

[27] Ceperley, D. M. & Alder, B. J. *Phys. Rev. Lett.* **45**, 566–569 (1980).

[28] Perdew, J. P. & Zunger, A. *Phys. Rev. B* **23**, 5048–5079 (1981).

[29] Vosko, S. H., Wilk, L. & Nusair, M. *Can. J. Phys.* **58**, 1200–1211 (1980).

[30] Perdew, J. P., Burke, K. & Ernzerhof, M. *Phys. Rev. Lett.* **77**, 3865–3868 (1996).

[31] Perdew, J. P. & Constantin, L. A. . *Phys. Rev. B - Condens. Matter Mater. Phys.* **75**, 1–9 (2007).

[32] Chai, J. Da & Head-Gordon, M. *Phys. Chem. Chem. Phys.* **10**, 6615–6620 (2008).

[33] Boys, S. F. & A, P. R. S. L. *Proc. R. Soc. London. Ser. A. Math. Phys. Sci.* **200**, 542–554 (1950).

[34] Hehre, W. J., Stewart, R. F. & Pople, J. A. *J. Chem. Phys.* **51**, 2657–2664 (1969).

[35] Ditchfield, R., Hehre, W. J. & Pople, J. A. . *J. Chem. Phys.* **54**, 720–723 (1971).

[36] Gordon, M. S., Binkley, J. S., Pople, J. A., Pietro, I. W. J. & Hehre, W. J. **2657**, 2797–2803 (1982).

[37] Pérez-Rodríguez, M. *et al*. *J. Am. Chem. Soc.* **131**, 3650–3657 (2009).

[38] Braga, A. A. C., Ujaque, G. & Maseras, F. *Organometallics* **25**, 3647–3658 (2006).

[39] Hay, P. J. & Wadt, W. R. *J. Chem. Phys.* **82**, 270–283 (1985).

[40] Tomasi, J. & Persico, M. *Chem. Rev.* **94**, 2027–2094 (1994).

[41] Bartók, A. P., Payne, M. C., Kondor, R. & Csányi, G. *Phys. Rev. Lett.* **104**, 1–4 (2010).

[42] Lunghi, A. & Sanvito, S. . *Sci. Adv.* **5**, 1–8 (2019).

[43] A. Bartók, M.J. Gillan, F.R. Manby, G. Csányi, On representing chemical environments, Phys. Rev. B 87 (2013) 184115..

[44] Thompson, A. P., Swiler, L. P., Trott, C. R., Foiles, S. M. & Tucker, G. J. *J. Comput. Phys.* **285**, 316–330 (2015).

[45] Shenkin, P. S. & McDonald, D. Q. *J. Comput. Chem.* **15**, 899–916 (1994).

[46] Kelley, L. A., Gardner, S. P. & Sutcliffe, M. J. *Protein Eng.* **9**, 1063–1065 (1996).

[47] Ehlers, A. W. *et al.* *Chem. Phys. Lett.* **208**, 111–114 (1993).

[48] The fitsnap code is available at: https://github.com/lunghiale/fitsnap

[49] M. P. Allen and D.J. Tildesly, Computer Simulation of Liquids (Oxford Science Publications, New York, 1989), p78

[50] M. J. Frisch, G. W. Trucks, H. B. Schlegel, G. E. Scuseria, M. A. Robb, J. R. Cheeseman, G. Scalmani, V. Barone, G. A. Petersson, Gaussian 09, Revision A.02, Gaussian, Inc., Wallingford CT, 2016

[51] Zhenqin L. Harold. A. Scheraga. *Proc. Natl. Acad. Sci. USA.* Vol. 84, pp. 6611-6615, October 1987

[52] Roos, K. *et al.* *J. Chem. Theory Comput.* **15**, 1863–1874 (2019).

Appendix-A

Cartesian coordinates

[1a]

Pd 0.072557 -0.318194 0.642885	C 1.732295 0.356355 -3.855251	H 0.931357 -2.999889 1.084260
Br -0.803109 -3.993295 -1.107032	C 3.601352 -1.973703 1.497930	H 0.459754 -1.905357 3.266948
P -1.832224 0.828518 0.000717	C 4.573388 -1.438336 -0.638937	H -3.301106 -3.373105 0.379759
P 2.292986 0.092819 0.187062	C 5.525189 -2.438335 -0.450456	H 0.401442 2.390707 -0.873497
C -1.165556 -3.211626 0.600504	C 5.521289 -3.200504 0.713653	H -3.566205 1.655042 -2.333638
C -0.089751 -2.807188 1.394416	C 4.556686 -2.965006 1.691298	H -3.136480 3.150874 -4.247994
C -0.364500 -2.212356 2.630954	C 2.158995 2.453253 1.651600	H -0.938686 4.276859 -4.485127
C -2.482622 -3.065994 1.020071	C 4.407546 1.648258 1.324298	H 0.832781 3.893140 -2.780513
C -1.612657 1.928729 -1.461472	C 4.900185 2.751108 2.016429	H 1.011544 -0.809008 -2.196075
C -3.303360 -0.163505 -0.484979	C 4.024484 3.710294 2.519296	H 3.906560 2.217214 -1.249607
C -2.518628 1.982898 1.257757	C 2.652666 3.559327 2.336503	H 3.977116 2.891404 -3.620673
C 3.602832 -1.193182 0.335615	C -3.310737 3.088091 0.929957	H 2.581859 1.710404 -5.298251
C 3.031324 1.492142 1.127987	C -2.238561 1.724023 2.603014	H 1.110146 -0.157606 -4.581091
C 2.472778 0.637223 -1.563861	C -2.750771 2.545692 3.603698	H 2.841359 -1.796280 2.255975
C -0.380505 2.574096 -1.603312	C -3.817433 3.912632 1.929035	H 4.584892 -0.848165 -1.550119
C -2.603855 2.149714 -2.423049	C -3.540224 3.641507 3.267392	H 6.272289 -2.620595 -1.216968
C -2.360903 2.993266 -3.504415	C -4.499855 -0.164333 0.233683	H 6.263831 -3.979278 0.857266
C -1.128509 3.627132 -3.636087	C -3.162326 -1.046488 -1.563204	H 4.544820 -3.558361 2.600467
C -0.138512 3.419853 -2.679281	C -4.197774 -1.899564 -1.922774	H 1.087138 2.318346 1.524873
C 1.685729 -0.018668 -2.518269	C -5.532754 -1.033400 -0.115239	H 5.097434 0.903867 0.937327
C 3.298044 1.686573 -1.975342	C -5.386976 -1.900169 -1.193448	H 5.970140 2.861488 2.164015
C 3.335752 2.070043 -3.315042	C -2.734205 -2.481868 2.258439	H 4.411372 4.570056 3.057726
C 2.555370 1.406289 -4.256381	C -1.682589 -2.046180 3.058342	H 1.962929 4.297872 2.733309

H -3.524558 3.307853 -0.111791
H -1.609359 0.873918 2.855109
H -2.526438 2.335408 4.645024
H -4.427699 4.770226 1.662564
H -3.933743 4.288660 4.045374
H -4.627357 0.511625 1.073362
H -2.226751 -1.073221 -2.115864
H -4.070312 -2.578094 -2.760511
H -6.456820 -1.026048 0.455262
H -6.192865 -2.574488 -1.466250
H -3.761400 -2.349278 2.580827
H -1.883258 -1.582553 4.018800

TS1

Pd -0.025854 -0.958089 -0.260226
Br -0.035184 -3.067752 -1.795493
P -1.727007 0.723690 -0.120415
P 2.161289 0.005284 0.038244
C -1.206498 -2.695401 0.037231
C -0.597443 -3.197297 1.196068
C -1.400333 -3.618989 2.261552
C -2.601536 -2.746098 -0.109511
C -1.292800 2.449889 -0.577819
C -3.165273 0.370266 -1.203396
C -2.463359 0.968853 1.543972
C 3.613025 -0.980283 -0.502475
C 2.514639 0.326112 1.813150
C 2.452440 1.629996 -0.761666
C -0.355424 3.124556 0.215222
C -1.828374 3.100693 -1.690183
C -1.438457 4.402561 -2.000862
C -0.518650 5.068297 -1.199770
C 0.021517 4.425305 -0.087504
C 1.835321 1.851197 -1.997434
C 3.245857 2.636947 -0.206502
C 3.430093 3.839598 -0.883634
C 2.821320 4.046234 -2.117960
C 2.022068 3.050672 -2.673923
C 3.517924 -2.372017 -0.401371
C 4.791633 -0.414844 -0.998840
C 5.859667 -1.227504 -1.370166
C 5.761861 -2.610837 -1.249085
C 4.588526 -3.182351 -0.763948
C 1.426670 0.584463 2.655256
C 3.803640 0.322647 2.356013
C 3.998880 0.591096 3.708098
C 2.910561 0.864919 4.533064
C 1.622578 0.859760 4.004426
C -3.119425 2.148752 1.915931
C -2.354223 -0.069444 2.473185
C -2.899829 0.063573 3.747206
C -3.662674 2.280848 3.189238
C -3.554229 1.237547 4.107144
C -4.494626 0.585295 -0.834794
C -2.888301 -0.180238 -2.461194
C -3.919892 -0.492308 -3.339788
C -5.527885 0.260286 -1.710447
C -5.243805 -0.274747 -2.963419
C -3.375513 -3.174161 0.955698
C -2.783874 -3.602515 2.150766
H 0.482601 -3.275244 1.261647
H -0.926545 -3.987080 3.166651
H -3.062764 -2.416666 -1.032630
H 0.085740 2.628475 1.075567
H -2.558425 2.597044 -2.315389
H -1.864706 4.896010 -2.869046
H -0.217531 6.083093 -1.440770
H 0.753813 4.930313 0.533657
H 1.187216 1.083637 -2.412734
H 3.716603 2.486059 0.760359
H 4.047436 4.616915 -0.443470
H 2.958090 4.988407 -2.639747
H 1.526891 3.216018 -3.625112
H 2.589925 -2.820805 -0.058974
H 4.874925 0.662542 -1.103968
H 6.767874 -0.777527 -1.759266
H 6.594039 -3.243148 -1.542995
H 4.498119 -4.260710 -0.680807
H 0.418113 0.549771 2.252258
H 4.656714 0.099394 1.721731
H 5.003525 0.581111 4.119601
H 3.066708 1.070060 5.587633

H 0.764962 1.057491 4.640102
H -3.196980 2.968392 1.207602
H -1.834811 -0.982826 2.202435
H -2.808642 -0.753828 4.455731
H -4.168029 3.200755 3.466774
H -3.977743 1.343902 5.101259
H -4.727196 0.997839 0.141592
H -1.857330 -0.393083 -2.734511
H -3.690897 -0.923301 -4.309146
H -6.558350 0.424747 -1.410800
H -6.051027 -0.530727 -3.642620
H -4.456684 -3.170303 0.855120
H -3.403919 -3.945867 2.972316

[1b]

Pd -0.221659 -1.182765 0.049164
Br 0.783137 -3.445303 -0.332679
P -1.524794 0.772891 -0.024674
P 1.977384 -0.118510 0.056881
C -1.972318 -2.220688 0.219196
C -2.230665 -2.818633 1.457513
C -3.388910 -3.562341 1.667126
C -2.872440 -2.441290 -0.821988
C -0.742202 2.426930 -0.286954
C -2.661028 0.628267 -1.449392
C -2.563227 1.161538 1.430509
C 3.503964 -1.126773 -0.053740
C 2.335808 0.825423 1.587227
C 2.142657 1.021592 -1.364305
C -0.166954 3.069170 0.815883
C -0.728208 3.077888 -1.522282
C -0.152205 4.338812 -1.649360
C 0.426999 4.963134 -0.550644
C 0.420709 4.321236 0.684618
C 1.731884 0.497789 -2.598097
C 2.653068 2.317229 -1.310195
C 2.763035 3.074151 -2.474122
C 2.362105 2.547735 -3.697081
C 1.842200 1.256306 -3.757858
C 3.707696 -2.100235 0.930312
C 4.474630 -0.932878 -1.036817
C 5.637423 -1.701213 -1.033158
C 5.837781 -2.661668 -0.048528
C 4.870394 -2.858541 0.935209
C 1.396053 0.816731 2.620193
C 3.558300 1.476834 1.789512
C 3.806212 2.155226 2.977084
C 2.847840 2.166675 3.989343
C 1.647086 1.486508 3.815166
C -3.346320 2.323727 1.454677
C -2.533486 0.337507 2.554659
C -3.285403 0.657531 3.683155
C -4.101809 2.637497 2.576702
C -4.072346 1.803126 3.693822
C -4.048996 0.669666 -1.328614
C -2.090100 0.354533 -2.698774
C -2.895203 0.158254 -3.813898
C -4.854300 0.457999 -2.445242
C -4.282015 0.207846 -3.687493
C -4.031720 -3.189967 -0.615756
C -4.302190 -3.742224 0.631296
H -1.506810 -2.736097 2.264838
H -3.567414 -4.016843 2.637854
H -2.679980 -2.038565 -1.810274
H -0.191686 2.600992 1.792504
H -1.175502 2.616669 -2.394087
H -0.153146 4.828191 -2.617930
H 0.878632 5.944798 -0.654984
H 0.864606 4.795251 1.554315
H 1.335917 -0.514967 -2.644951
H 2.940686 2.753718 -0.360470
H 3.153540 4.085328 -2.417617
H 2.449674 3.141677 -4.601521
H 1.526115 0.836769 -4.707819
H 2.947113 -2.275205 1.684586
H 4.331599 -0.183465 -1.808185
H 6.386094 -1.544685 -1.803556
H 6.743937 -3.259611 -0.047991
H 5.014730 -3.614626 1.700088
H 0.457347 0.285886 2.485320
H 4.325145 1.435339 1.021414
H 4.755050 2.662484 3.120192

H 3.046381 2.689788 4.919575
H 0.903272 1.473542 4.605470
H -3.355274 2.988888 0.595943
H -1.933800 -0.564269 2.540266
H -3.257218 0.004105 4.549151
H -4.708294 3.537594 2.583820
H -4.660018 2.051516 4.572142
H -4.509796 0.836255 -0.361510
H -1.010554 0.272949 -2.794106
H -2.440081 -0.052137 -4.776297
H -5.933904 0.478899 -2.336637
H -4.913150 0.038680 -4.554109
H -4.722040 -3.342166 -1.441040
H -5.206293 -4.322026 0.791280

[2a]

Pd 1.694957 -0.741350 -1.050041
N -1.371166 -1.369175 -1.059891
N -0.861692 0.414372 0.065463
C -0.310987 -0.649193 -0.603400
C -2.234916 0.355346 0.013458
C -2.556028 -0.767646 -0.692487
C 1.198378 1.846391 2.775155
H 1.504101 1.625068 3.791822
C 0.287116 1.033007 2.116874
C 0.561847 2.391465 0.102679
C 1.470405 3.200821 0.786355
H 1.952520 4.008501 0.251477
C -0.028672 1.328531 0.783720
C -1.216671 -2.575388 -1.814925
C -3.450148 1.050710 0.426711
C 0.609788 -0.800196 3.820059
C 1.795638 2.919977 2.111428
C -0.326158 -0.194132 2.784280
H -0.418774 -0.952075 2.002794
C -1.167397 3.210444 -1.514907
C -4.492903 0.223844 -0.081644
C -4.002571 -0.918178 -0.778101
C 0.231330 2.633043 -1.369150
H 0.202948 1.643836 -1.847500
C 1.333452 3.401520 -2.089304
C -3.782894 2.190129 1.106809
H -3.024628 2.853307 1.505522
C -5.848337 0.497038 0.084935
C 0.434636 -0.662735 5.194824
H -0.429150 -0.130709 5.580813
C -1.276306 -3.793806 -1.129901
C -1.490399 -3.832107 0.374619
H -2.043877 -2.927452 0.648749
C -2.067398 1.255682 3.954731
H -1.304403 2.012697 4.114581
C 2.586255 2.785597 -2.208553
H 2.744759 1.787768 -1.806980
C 1.717355 -1.508310 3.345825
H 1.849688 -1.623474 2.274007
C -2.074158 2.630985 -2.403545
H -1.765744 1.771517 -2.993721
C -4.896354 -1.811106 -1.311505
H -4.564806 -2.696535 -1.845329
C -3.369608 1.477093 4.395416
H -3.612829 2.402156 4.909466
C -1.734584 0.075342 3.288273
C -5.162518 2.495290 1.282644
H -5.422600 3.399569 1.823870
C 3.642322 3.437582 -2.829862
H 4.605945 2.942760 -2.902531
C -0.809919 -4.888866 -3.238683
H -0.644582 -5.804301 -3.798592
C -6.757792 -0.444095 -0.477134
H -7.827532 -0.285764 -0.374325
C -1.583463 4.305522 -0.753545
H -0.892399 4.756068 -0.046022
C -1.064452 -4.953928 -1.872988
H -1.086809 -5.919487 -1.379404
C -2.333725 -5.022774 0.837460
H -3.285011 -5.079296 0.299210
H -2.549923 -4.926424 1.905779
H -1.808253 -5.973438 0.700573
C 1.160438 4.678786 -2.617460
H 0.195200 5.169314 -2.544897
C -6.167196 1.688359 0.800606
H -7.207449 1.955603 0.963365

C -6.286239 -1.552895 -1.145836
H -6.995859 -2.260008 -1.563931
C 2.639127 -2.059895 4.224588
H 3.492965 -2.605882 3.834483
C -0.968615 -2.472894 -3.187663
C -0.767548 -3.663141 -3.889390
H -0.575006 -3.626810 -4.957605
C 3.462321 4.718065 -3.353311
H 4.286364 5.229529 -3.841246
C 2.220408 5.332570 -3.247368
H 2.068087 6.326292 -3.657949
C -4.038057 -0.651557 3.495409
H -4.805013 -1.392397 3.293586
C 2.464514 -1.911036 5.599971
H 3.183434 -2.338166 6.292189
C 1.360708 -1.214944 6.080086
H 1.213576 -1.098927 7.149510
C -0.930189 -1.134158 -3.904002
H -1.037001 -0.351610 -3.147809
C -2.732255 -0.877409 3.074517
H -2.483421 -1.797979 2.552071
C -0.140989 -3.789299 1.103510
H 0.449440 -4.684052 0.880482
H -0.283890 -3.725317 2.187355
H 0.449479 -2.929297 0.782671
C 0.414849 -0.901532 -4.600832
H 1.234536 -0.954045 -3.875597
H 0.434500 0.088891 -5.063679
H 0.598486 -1.644096 -5.384793
C -2.111690 -0.999473 -4.872890
H -2.065006 -1.756871 -5.662624
H -2.102765 -0.014991 -5.351841
H -3.065303 -1.117355 -4.348428
C -4.360272 0.528551 4.159664
H -5.380647 0.712696 4.479994
C -3.370060 3.123806 -2.525163
H -4.066610 2.644438 -3.205526
C -3.772125 4.219243 -1.767505
H -4.783680 4.602262 -1.855485
C -2.872720 4.812536 -0.885444
H -3.179956 5.664888 -0.286878
C 2.683318 -2.464074 -0.708629
C 2.459297 -3.443215 -1.668996
C 3.326199 -2.777495 0.490084
C 2.684150 -4.776955 -1.344242
H 2.019420 -3.184226 -2.628461
C 3.542926 -4.118299 0.808431
H 3.624170 -1.993603 1.178937
C 3.190344 -5.121897 -0.092327
H 2.429996 -5.552247 -2.065097
H 3.986603 -4.376894 1.764094
H 3.338845 -6.165085 0.167882
H 4.091491 -1.238050 -2.221517
N 3.654855 -0.636532 -1.510775
C 4.573875 -0.127998 -0.633247
C 5.960173 -0.194175 -0.880631
C 4.148955 0.549915 0.529404
C 6.858936 0.451389 -0.045494
H 6.315958 -0.733177 -1.757452
C 5.059431 1.168833 1.369298
H 3.084087 0.597655 0.749948
C 6.423343 1.140686 1.084878
H 7.922113 0.407570 -0.276332
H 4.693743 1.675850 2.258176
H 7.136547 1.639245 1.734163
O 2.709548 3.622271 2.824544
C 3.519223 4.553996 2.126334
H 4.248190 4.913991 2.850210
H 4.038706 4.069183 1.292435
H 2.930216 5.398920 1.755486

TS2

Pd 1.679360 -0.734069 -1.048209
N -1.366565 -1.372242 -1.058222
N -0.866461 0.414676 0.064676
C -0.308972 -0.642025 -0.608438
C -2.239481 0.347980 0.015280
C -2.553567 -0.777059 -0.689100
C 1.190791 1.854575 2.772990
H 1.496865 1.635801 3.790135
C 0.282473 1.037171 2.115555
C 0.553412 2.396617 0.099526

C 1.458970 3.206952 0.782276
H 1.938594 4.015478 0.246372
C -0.036778 1.332657 0.781894
C -1.207811 -2.579004 -1.811381
C -3.457235 1.039918 0.424144
C 0.610729 -0.792435 3.821617
C 1.784699 2.929156 2.107883
C -0.326908 -0.190994 2.784649
H -0.416725 -0.950366 2.001221
C -1.178036 3.204443 -1.519886
C -4.496960 0.208822 -0.083430
C -3.999579 -0.932581 -0.777986
C 0.222553 2.631944 -1.372796
H 0.203684 1.641888 -1.843749
C 1.322368 3.402980 -2.093703
C -3.791044 2.179213 1.102370
H -3.035080 2.845539 1.500414
C -5.850393 0.477726 0.082320
C 0.434616 -0.653534 5.196135
H -0.431145 -0.123771 5.580966
C -1.263640 -3.799646 -1.124564
C -1.478084 -3.836437 0.379885
H -2.034652 -2.933230 0.652529
C -2.073437 1.254689 3.952332
H -1.313019 2.014532 4.111266
C 2.577338 2.791062 -2.211649
H 2.730021 1.794355 -1.802474
C 1.720810 -1.497493 3.348812
H 1.853890 -1.613782 2.277196
C -2.082498 2.620640 -2.407962
H -1.771008 1.761298 -2.996755
C -4.890166 -1.829327 -1.310381
H -4.555482 -2.714409 -1.842752
C -3.376462 1.472416 4.392180
H -3.623013 2.397388 4.904818
C -1.736370 0.074539 3.287662
C -5.171747 2.479994 1.277347
H -5.434975 3.384156 1.817143
C 3.631380 3.445704 -2.833528
H 4.596706 2.953974 -2.905130
C -0.792773 -4.896250 -3.231562
H -0.624248 -5.811939 -3.790136
C -6.756512 -0.467298 -0.478672
H -7.826840 -0.312391 -0.376506
C -1.598032 4.299157 -0.760305
H -0.908716 4.753077 -0.053183
C -1.047616 -4.960059 -1.865940
H -1.066943 -5.925022 -1.370935
C -2.317596 -5.029218 0.844167
H -3.268542 -5.086683 0.305711
H -2.534513 -4.932016 1.912334
H -1.788877 -5.978344 0.708947
C 1.145331 4.678886 -2.623789
H 0.178394 5.166264 -2.552296
C -6.173463 1.669007 0.796130
H -7.214717 1.933003 0.958125
C -6.281029 -1.575497 -1.145641
H -6.988101 -2.285562 -1.562936
C 2.644059 -2.044698 4.228705
H 3.499926 -2.588359 3.839655
C -0.959645 -2.480744 -3.184187
C -0.754312 -3.671276 -3.884053
H -0.561499 -3.635854 -4.952333
C 3.447279 4.724769 -3.358858
H 4.269781 5.238344 -3.847266
C 2.203251 5.335300 -3.254343
H 2.047759 6.327869 -3.666426
C -4.037468 -0.659794 3.495088
H -4.801924 -1.403467 3.294075
C 2.468481 -1.894429 5.603776
H 3.188626 -2.318137 6.296871
C 1.362216 -1.201253 6.082471
H 1.214332 -1.084167 7.151701
C -0.925370 -1.142869 -3.902460
H -1.032147 -0.359588 -3.147503
C -2.730759 -0.881930 3.075015
H -2.478669 -1.802369 2.554036
C -0.126058 -3.787998 1.106174
H 0.461352 -4.687091 0.893716
H -0.269636 -3.713881 2.189860
H 0.467644 -2.932543 0.775255

C 0.419123 -0.906775 -4.599184
H 1.235743 -0.952467 -3.870595
H 0.435625 0.083022 -5.066545
H 0.605507 -1.649939 -5.381978
C -2.106978 -1.013584 -4.872005
H -2.057468 -1.772027 -5.660642
H -2.101248 -0.029752 -5.352441
H -3.060399 -1.133860 -4.347715
C -4.363912 0.520150 4.157469
H -5.384955 0.701425 4.477224
C -3.379965 3.108937 -2.530751
H -4.074683 2.626236 -3.210670
C -3.786019 4.204147 -1.774870
H -4.798842 4.583567 -1.863752
C -2.888864 4.801708 -0.893391
H -3.199173 5.653934 -0.296194
C 2.841406 -2.395994 -0.748929
C 2.527995 -3.401337 -1.677938
C 3.379890 -2.753472 0.492525
C 2.691226 -4.739793 -1.333065
H 2.111589 -3.142234 -2.646876
C 3.540972 -4.096140 0.818885
H 3.693007 -1.982574 1.189331
C 3.192089 -5.099242 -0.083535
H 2.406923 -5.504973 -2.049877
H 3.952241 -4.357771 1.790099
H 3.320000 -6.144540 0.178340
H 4.080961 -1.203514 -2.260099
N 3.657105 -0.776379 -1.448393
C 4.577065 -0.149482 -0.613340
C 5.954736 -0.184355 -0.881066
C 4.140450 0.549672 0.527227
C 6.854034 0.477353 -0.052611
H 6.315610 -0.732460 -1.748020
C 5.048571 1.184950 1.363459
H 3.075431 0.588223 0.744278
C 6.412738 1.163874 1.076605
H 7.914392 0.442770 -0.285985
H 4.677906 1.701036 2.245501
H 7.120955 1.668817 1.725399
O 2.699015 3.635641 2.820301
C 3.502801 4.568950 2.121044
H 4.230299 4.935491 2.844624
H 4.024207 4.087677 1.284958
H 2.908120 5.411352 1.748669

[2b]

Pd 1.527381 -0.719652 -1.233419
N -1.495968 -1.221029 -1.288458
N -0.898234 0.346574 0.088508
C -0.393639 -0.528398 -0.853238
C -2.255527 0.176255 0.240853
C -2.629356 -0.808668 -0.619253
C 1.262675 1.454376 2.876656
H 1.685967 1.077837 3.802251
C 0.419293 0.662402 2.109252
C 0.337752 2.421862 0.417392
C 1.158853 3.213997 1.217382
H 1.471872 4.179499 0.842241
C -0.053372 1.170735 0.891779
C -1.444091 -2.324460 -2.195585
C -3.418888 0.680990 0.962382
C 1.166790 -1.499475 3.183926
C 1.617920 2.730848 2.439916
C 0.016689 -0.742764 2.536331
H -0.189857 -1.283408 1.610720
C -1.586760 3.196576 -0.989100
C -4.494644 -0.097803 0.446789
C -4.065415 -1.037430 -0.536904
C -0.104612 2.863147 -0.974645
H 0.031593 1.979838 -1.610534
C 0.806784 3.934055 -1.559087
C -3.681187 1.616478 1.924583
H -2.893313 2.225946 2.352203
C -5.813566 0.034419 0.862421
C 1.319994 -1.633215 4.562282
H 0.576837 -1.210879 5.232173
C -1.100800 -3.584297 -1.691106
C -0.819239 -3.811334 -0.215746
H -0.797921 -2.834114 0.271262
C -1.552120 0.202960 4.318967
H -0.811704 0.962710 4.552003

C 2.141914 3.590944 -1.811875	C 0.382317 5.229097 -1.848524	H 0.746816 -4.545519 1.091627
H 2.484575 2.583954 -1.581237	H -0.650867 5.509569 -1.671993	H 1.337514 -3.798900 -0.399887
C 2.117276 -2.079282 2.335923	C -6.062818 1.020544 1.861740	C -0.823537 0.041623 -4.443671
H 1.993931 -1.978790 1.256652	H -7.073973 1.172140 2.229119	H -0.096108 0.059338 -3.624757
C -2.424346 2.597086 -1.929619	C -6.353220 -1.740817 -0.707574	H -1.053536 1.072876 -4.735026
H -1.995236 1.912601 -2.656132	H -7.089725 -2.393660 -1.165722	H -0.354534 -0.454949 -5.300671
C -4.994402 -1.863011 -1.116471	C 3.201855 -2.775376 2.855091	C -3.138679 -0.689567 -5.159885
H -4.713209 -2.595103 -1.867442	H 3.920599 -3.225804 2.177496	H -2.738805 -1.110118 -6.088634
C -2.771450 0.199477 4.991206	C -1.760827 -2.100391 -3.542392	H -3.435343 0.341611 -5.375051
H -2.964937 0.944813 5.756888	C -1.701768 -3.192539 -4.407168	H -4.035982 -1.253503 -4.887077
C -1.284197 -0.740872 3.326008	H -1.929852 -3.058979 -5.459493	C -3.747031 -0.738990 4.669353
C -5.026331 1.773417 2.364195	C 2.594855 5.820343 -2.616212	H -4.707028 -0.725172 5.175357
H -5.233516 2.515108 3.129240	H 3.286954 6.551053 -3.023734	C -3.795058 2.836432 -1.921706
C 3.026823 4.524598 -2.333552	C 1.271576 6.167080 -2.373711	H -4.433615 2.334079 -2.641894
H 4.057353 4.238033 -2.516675	H 0.921709 7.171365 -2.593556	C -4.344712 3.704533 -0.982911
C -1.350675 -4.453954 -3.937933	C -3.489996 -1.684835 3.680938	H -5.414882 3.883610 -0.964843
H -1.311726 -5.292477 -4.626768	H -4.248518 -2.411181 3.407225	C -3.515278 4.325607 -0.053434
C -6.761247 -0.831963 0.243988	C 3.354080 -2.895829 4.235597	H -3.936776 4.998875 0.686903
H -7.809153 -0.772590 0.524506	H 4.200066 -3.438441 4.646463	C 4.297462 -2.064970 -1.031430
C -2.148239 4.064954 -0.050372	C 2.412641 -2.324189 5.085119	C 3.744384 -3.235237 -1.559859
H -1.508534 4.525379 0.698324	H 2.521310 -2.422733 6.161044	C 5.352845 -2.147655 -0.126624
C -1.059555 -4.647923 -2.594339	C -2.102920 -0.703219 -4.032671	C 4.243615 -4.473415 -1.182021
H -0.801171 -5.640806 -2.237528	H -2.546227 -0.164043 -3.188929	H 2.898503 -3.157839 -2.238324
C -1.948710 -4.624904 0.429375	C -2.264878 -1.688233 3.023752	C 5.840673 -3.397762 0.253890
H -2.913457 -4.120481 0.307614	H -2.076794 -2.416314 2.239334	H 5.791035 -1.247855 0.288421
H -1.761959 -4.757884 1.500286	C 0.556924 -4.440010 0.018853	C 5.292199 -4.563382 -0.266567
H -2.029943 -5.619496 -0.022625	H 0.637676 -5.433084 -0.437275	H 3.796985 -5.373448 -1.592375

H 6.657889 -3.450083 0.966644	C -0.500157 3.943984 0.691175	C 2.920456 1.345936 2.101727
H 5.673816 -5.532553 0.037203	H -0.809801 4.680989 -0.053070	C 4.185668 0.780991 2.221336
H 3.794636 -0.760498 -2.482677	H -0.964844 4.196459 1.649827	H 4.521068 0.447364 3.200541
N 3.743412 -0.804163 -1.467843	C 1.021426 3.794377 0.790738	C 5.036202 0.643072 1.122152
C 4.296241 0.398194 -0.905473	H 1.429266 4.164873 1.733749	C 4.604238 1.103210 -0.116408
C 5.112786 1.221966 -1.676212	H 1.546289 4.285992 -0.035605	H 5.254139 0.999287 -0.980912
C 4.007543 0.740501 0.417262	C -2.283351 2.347190 -0.100810	C 3.340619 1.668134 -0.292766
C 5.635603 2.392566 -1.129226	C -2.691148 2.620612 -1.411931	C 2.051587 1.563711 3.311023
H 5.338814 0.950463 -2.704098	C -4.019927 2.356721 -1.746781	H 2.511823 1.125875 4.199187
C 4.552916 1.895103 0.963288	H -4.346204 2.539540 -2.767757	H 1.911643 2.634050 3.503402
H 3.352881 0.104870 1.005389	C -4.933437 1.879555 -0.810916	H 1.068194 1.107932 3.178576
C 5.361320 2.729422 0.191420	C -4.505717 1.697319 0.505111	C 6.398079 0.021821 1.290335
H 6.267871 3.031938 -1.737587	H -5.218004 1.361925 1.254611	H 6.892458 -0.117080 0.326161
H 4.332288 2.146397 1.995860	C -3.187072 1.926085 0.886038	H 7.040656 0.648696 1.917612
H 5.777279 3.635605 0.620385	C -1.777402 3.252251 -2.428869	H 6.321749 -0.956664 1.774935
O 2.459302 3.425445 3.255695	H -0.724626 3.118844 -2.180672	C 2.942088 2.214872 -1.637589
C 2.942771 4.672297 2.796815	H -1.931109 2.806816 -3.413917	H 3.135478 3.293461 -1.685677
H 3.639932 5.021731 3.558075	H -1.991436 4.325250 -2.506838	H 3.526564 1.739193 -2.428113
H 3.465783 4.566211 1.838218	C -6.352776 1.559169 -1.202000	H 1.888602 2.041000 -1.863577
H 2.131640 5.401773 2.685915	H -6.477737 0.479779 -1.339343	C 1.414824 -1.687484 -0.229695
[3a]	H -7.059215 1.874584 -0.428930	H 1.521687 -2.099907 0.773941
Ru 0.071963 -0.252686 -0.223262	H -6.629777 2.048157 -2.139344	C 2.715521 -1.701479 -0.946784
Cl -0.011882 0.421514 -2.548117	C -2.751595 1.750930 2.316167	C 3.811576 -2.223082 -0.246900
Cl -0.203064 -0.829124 2.111123	H -3.599251 1.466332 2.943086	H 3.676919 -2.562880 0.776178
N -0.924376 2.600358 0.272523	H -1.986355 0.975280 2.409786	C 5.063839 -2.312166 -0.843931
N 1.200259 2.340044 0.691884	H -2.335570 2.680089 2.721732	H 5.898426 -2.728372 -0.288704
C 0.074056 1.716686 0.323570	C 2.498777 1.747324 0.823399	C 5.244469 -1.861918 -2.147938

H 6.221004 -1.927727 -2.617853
C 4.163313 -1.331703 -2.850047
H 4.297136 -0.975835 -3.867026
C 2.907900 -1.253833 -2.259590
H 2.074415 -0.821949 -2.802061
C -1.223608 -1.675465 -0.702160
C 0.153874 -2.369022 -0.961403
H -1.709188 -1.422209 -1.648687
H 0.352044 -2.436197 -2.029239
H 0.143739 -3.346588 -0.476062
Si -2.425066 -2.615389 0.386592
Cl -1.552587 -4.062626 1.552766
Cl -3.606334 -3.646387 -0.969045
Cl -3.716177 -1.507046 1.510506

TS3

Ru -0.137458 0.395130 -0.332450
Cl -0.234902 -0.358043 -2.655466
Cl -0.022833 1.062162 1.991145
N 0.764241 -2.516137 -0.058213
N -1.351937 -2.266405 0.387637
C -0.214906 -1.616971 0.108029
C 0.309155 -3.895266 0.160048
H 0.584092 -4.519834 -0.693366
H 0.782587 -4.306624 1.058232
C -1.205795 -3.725030 0.311584
H -1.605161 -4.193422 1.214701
H -1.758907 -4.105805 -0.552968
C 2.156342 -2.240147 -0.226738
C 2.749981 -2.377567 -1.486185
C 4.106339 -2.067892 -1.602401
H 4.576845 -2.145664 -2.579629
C 4.870439 -1.680637 -0.504569
C 4.259321 -1.639571 0.749829
H 4.852145 -1.378183 1.622185
C 2.904543 -1.913849 0.914123
C 1.997871 -2.910601 -2.676238
H 0.921965 -2.776297 -2.571144
H 2.300274 -2.394391 -3.590187
H 2.216596 -3.977372 -2.808167
C 6.320959 -1.305028 -0.659578
H 6.425236 -0.218026 -0.747182
H 6.908531 -1.622480 0.206417
H 6.758017 -1.754628 -1.554889
C 2.258287 -1.873264 2.274070
H 3.010362 -1.731282 3.052689
H 1.536444 -1.053427 2.348398
H 1.724652 -2.805149 2.490332
C -2.615622 -1.680110 0.714733
C -2.880845 -1.401787 2.065926
C -4.124967 -0.870761 2.389648
H -4.340157 -0.634278 3.428975
C -5.103555 -0.652162 1.418372
C -4.822125 -0.991197 0.099501
H -5.576819 -0.832909 -0.665539
C -3.584375 -1.509262 -0.281483
C -1.861037 -1.692933 3.133977
H -2.292783 -1.544922 4.126158
H -1.502176 -2.726330 3.074011
H -0.997043 -1.030926 3.034886
C -6.439199 -0.070199 1.802692
H -7.059850 0.115849 0.922536
H -6.989068 -0.744869 2.466984
H -6.312612 0.878175 2.334904
C -3.342527 -1.914797 -1.710761
H -3.545109 -2.984313 -1.846661
H -4.009365 -1.364556 -2.378060
H -2.317450 -1.715362 -2.029450
C -1.177808 2.297612 -0.532904
H -1.129312 2.771077 0.444723
C -2.566534 2.062278 -0.996239
C -3.585049 2.304501 -0.065014
H -3.320282 2.554029 0.958460
C -4.920744 2.239322 -0.441571
H -5.696641 2.442933 0.289397
C -5.258651 1.903204 -1.748485
H -6.301706 1.850887 -2.045770
C -4.252907 1.627942 -2.673617
H -4.508926 1.358409 -3.693510
C -2.915639 1.710482 -2.306480
H -2.142230 1.488156 -3.032384
C 1.528132 1.107964 -0.631244

C -0.036162 2.484299 -1.344972
H 1.977529 0.902489 -1.612708
H -0.066486 2.267803 -2.407469
H 0.657358 3.254728 -1.032372
Si 2.714610 2.082646 0.498494
Cl 2.031878 3.967525 0.963537
Cl 4.363889 2.352415 -0.726822
Cl 3.454873 1.291241 2.226786

[3b]

Ru 0.154042 -0.433899 -0.481301
Cl 0.189286 0.428909 -2.770253
Cl 0.288087 -1.211065 1.813335
N -0.958344 2.420602 -0.130016
N 1.177470 2.263433 0.263400
C 0.067417 1.559138 -0.005046
C -0.561458 3.812602 0.117827
H -0.903556 4.454035 -0.697010
H -1.012642 4.167070 1.051651
C 0.962045 3.712869 0.195321
H 1.384234 4.199553 1.077881
H 1.453319 4.115611 -0.696307
C -2.349287 2.102941 -0.173429
C -3.067453 2.275286 -1.362907
C -4.422054 1.941215 -1.357491
H -4.988078 2.045813 -2.279735
C -5.065207 1.483324 -0.208838
C -4.330694 1.391905 0.973874
H -4.825816 1.068733 1.885514
C -2.972947 1.702570 1.018101
C -2.420571 2.831976 -2.601968
H -1.414016 2.431941 -2.738853
H -3.008569 2.586157 -3.489087
H -2.357206 3.925570 -2.543506
C -6.516189 1.081411 -0.240647
H -6.605796 -0.001822 -0.376119
H -7.021205 1.338770 0.694381
H -7.047231 1.565754 -1.064092
C -2.195202 1.623706 2.305445
H -2.862682 1.426718 3.146127
H -1.449317 0.823151 2.274371
H -1.664246 2.559841 2.508250
C 2.464316 1.758688 0.634240
C 2.704460 1.514451 1.996240
C 3.971312 1.074445 2.366615
H 4.166507 0.859624 3.414395
C 4.995299 0.920754 1.431902
C 4.736164 1.235191 0.102148
H 5.529913 1.141609 -0.633010
C 3.478494 1.658524 -0.325356
C 1.637569 1.746976 3.032144
H 2.060991 1.684390 4.036887
H 1.176197 2.734465 2.921235
H 0.849373 0.995235 2.947037
C 6.364155 0.462344 1.863363
H 6.932852 0.067329 1.017537
H 6.936871 1.290939 2.294147
H 6.296528 -0.320178 2.624546
C 3.260307 2.050817 -1.761762
H 3.388176 3.132963 -1.887213
H 3.993476 1.558523 -2.404535
H 2.264682 1.780544 -2.119986
C 1.376420 -2.511870 -0.788270
H 1.129989 -3.016170 0.141311
C 2.789094 -2.094858 -0.922052
C 3.662340 -2.393657 0.131332
H 3.257349 -2.799222 1.053689
C 5.031209 -2.202711 -0.010340
H 5.699375 -2.458387 0.805778
C 5.542748 -1.689646 -1.198440
H 6.613372 -1.551399 -1.316257
C 4.676509 -1.333561 -2.230298
H 5.069330 -0.909273 -3.149183
C 3.308056 -1.528659 -2.095168
H 2.641727 -1.244285 -2.903543
C -1.613238 -0.778543 -0.530081
C 0.455497 -2.520844 -1.791649
H -2.199043 -0.328527 -1.344256
H 0.667166 -2.147738 -2.785918
H -0.472861 -3.062109 -1.665932
Si -2.623679 -2.031778 0.477273
Cl -1.788083 -3.908889 0.504300

Cl -4.370315 -2.218829 -0.619616

Cl -3.205685 -1.601170 2.388274

[4a]

Ru 0.074334 -0.099953 -1.203424

O 0.334329 1.200892 -3.865144

C 0.242619 0.737431 -2.789584

P -1.641890 1.218635 -0.447725

P 2.240939 0.340072 -0.582483

O 0.376516 0.957513 1.680135

C -1.950772 0.755934 1.316918

C -3.205882 0.414252 1.828196

H -4.076902 0.489809 1.185913

C -3.343156 -0.037648 3.136761

H -4.324664 -0.305068 3.515311

C -2.231867 -0.140486 3.968721

H -2.362002 -0.490584 4.986787

C -0.964038 0.209506 3.507627

C 0.306064 0.236476 4.354974

C 1.465718 -0.197618 3.458804

C 2.571655 -0.928157 3.888578

H 2.624427 -1.285507 4.911119

C 3.625664 -1.191232 3.019139

H 4.490002 -1.745521 3.370959

C 3.576760 -0.753444 1.700612

H 4.392320 -0.994970 1.028834

C 2.473441 -0.045700 1.214991

C 1.449104 0.226838 2.129611

C -0.855696 0.637508 2.184650

C 0.185005 -0.640352 5.603766

H 0.010825 -1.689387 5.346763

H -0.635486 -0.296337 6.239071

H 1.092682 -0.575922 6.209300

C 0.557589 1.701057 4.791727

H 1.490436 1.769111 5.360154

H -0.265854 2.053917 5.420829

H 0.635013 2.363985 3.925175

C 3.792329 -0.355043 -1.300049

C 5.041244 0.269745 -1.196073

C 3.701011 -1.583332 -1.955567

C 6.175175 -0.331387 -1.731257

H 5.123711 1.229881 -0.695014

C 4.836822 -2.188723 -2.487197

H 2.730136 -2.062748 -2.045233

C 6.074345 -1.563680 -2.376228

C 2.833643 2.693667 -1.952602

C 2.848437 4.351796 0.274967

H 2.436562 2.585549 1.417558

C 3.082445 4.052301 -2.100293

H 2.820439 2.054605 -2.831026

C 3.089894 4.887109 -0.984724

H 2.839361 4.996471 1.148447

H 3.262769 4.461070 -3.089816

H 3.273927 5.950848 -1.100584

C -3.361518 1.376186 -1.096274

C -4.199497 2.455965 -0.792542

C -3.833510 0.363921 -1.933680

C -5.486348 2.516098 -1.314485

H -3.838965 3.254050 -0.150283

C -5.120529 0.427888 -2.462805

H -3.179702 -0.471650 -2.173571

C -5.947324 1.502463 -2.153570

H -6.128263 3.358297 -1.074124

H -5.471174 -0.363521 -3.116712

H -6.947603 1.558007 -2.572717

C -1.170445 2.995926 -0.273180

C -0.640266 3.661456 -1.382684

C -1.335648 3.705605 0.919565

C -0.295035 5.005074 -1.302599

H -0.484464 3.127934 -2.313858

C -0.975164 5.048539 1.003278

H -1.749346 3.213336 1.794277

C -0.456809 5.702305 -0.108536

H 0.125563 5.499936 -2.171798

H -1.104058 5.580903 1.941065

H -0.173361 6.748465 -0.043799

C -0.428395 -2.926230 -0.185012

H -0.871920 -2.754177 -1.176050

O -0.301002 -1.663880 0.468779

H -1.153752 -1.465585 0.886599

C -1.354546 -3.804080 0.658489

H -1.529076 -4.769139 0.170386

H -0.884922 -3.985160 1.628832

O -2.566839 -3.133921 0.953666

C -3.564743 -3.084404 0.015250

C -3.481574 -3.634716 -1.262792

C -4.733293 -2.438851 0.425703

C -4.578879 -3.538217 -2.119828

H -2.586926 -4.138563 -1.607584

C -5.813015 -2.347675 -0.438422

H -4.767722 -2.020892 1.425219

C -5.744854 -2.901918 -1.716853

H -4.508126 -3.971557 -3.112486

H -6.713755 -1.836910 -0.113991

H 7.139044 0.161256 -1.646281

H 4.748199 -3.147779 -2.988043

H 6.960495 -2.029944 -2.796447

C 2.603714 2.143392 -0.685548

C 2.612203 2.987449 0.425639

H -6.591485 -2.831400 -2.391475

C 0.924034 -3.568854 -0.330673

C 1.215320 -4.333124 -1.460370

C 1.871388 -3.453344 0.686649

C 2.444159 -4.977136 -1.574506

H 0.483735 -4.410044 -2.261103

C 3.104786 -4.082191 0.563386

H 1.651272 -2.841639 1.555957

C 3.392768 -4.848463 -0.563302

H 2.665994 -5.564350 -2.460160

H 3.846026 -3.962649 1.347169

H 4.358922 -5.333253 -0.659848

TS4

Ru -0.063522 -0.058359 -1.190816

O -0.095380 1.374378 -3.813892

C -0.068987 0.872682 -2.758028

P -1.508950 1.386643 -0.265938

P 2.247572 0.339947 -0.591880

O 0.473484 0.813581 1.737750

C -1.856293 0.821388 1.441757

C -3.128769 0.553536 1.938088

H -3.999362 0.765817 1.326262

C -3.279614 -0.010578 3.201165

H -4.272696 -0.226514 3.581366

C -2.165279 -0.303376 3.981099

H -2.311150 -0.746176 4.960086

C -0.875903 -0.028059 3.525408

C 0.402626 -0.207640 4.343436

C 1.544154 -0.545301 3.382106

C 2.660834 -1.307213 3.722026

H 2.729078 -1.762078 4.703960

C 3.708865 -1.479397 2.822374

H 4.579357 -2.058806 3.112874

C 3.639890 -0.928608 1.548581

H 4.442025 -1.109276 0.841984

C 2.525987 -0.185116 1.152550

C 1.516961 0.010197 2.102428

C -0.762541 0.522621 2.254577

C 0.236467 -1.280311 5.425034

H 0.006157 -2.255563 4.987250

H -0.564016 -1.009595 6.117934

H 1.144442 -1.370905 6.026537

C 0.732374 1.146341 5.017874

H 1.665646 1.069688 5.584993

H -0.073143 1.435308 5.700373

H 0.849137 1.937497 4.271152

C 3.680849 -0.417045 -1.452355

C 4.949239 0.173237 -1.500841

C 3.483995 -1.659549 -2.059096

C 5.998381 -0.471356 -2.147290

H 5.113746 1.139636 -1.034259

C 4.536997 -2.307631 -2.697971

H 2.505325 -2.130212 -2.020227

C 5.793738 -1.713145 -2.746339

C 2.848985 2.729061 -1.874013

C 3.121325 4.245110 0.439479

H 2.667075 2.436866 1.506055

C 3.183188 4.074387 -1.961500

H 2.731288 2.145086 -2.782835

C 3.320700 4.836054 -0.802721

H 3.209087 4.836145 1.345532

H 3.326543 4.530989 -2.935885

H 3.569524 5.890589 -0.871221

C -3.170324 1.675372 -0.986540

C -3.903627 2.832731 -0.695808
C -3.724723 0.706595 -1.824898
C -5.170130 3.014027 -1.238786
H -3.481090 3.595081 -0.048542
C -4.991881 0.893036 -2.371203
H -3.157028 -0.192908 -2.046972
C -5.714001 2.045496 -2.081059
H -5.729518 3.916191 -1.011293
H -5.408610 0.130121 -3.020111
H -6.698663 2.193911 -2.514086
C -0.902724 3.106465 -0.016458
C -0.424394 3.821391 -1.118584
C -0.954766 3.738001 1.228816
C -0.022232 5.143787 -0.979784
H -0.362218 3.346791 -2.091717
C -0.539208 5.059943 1.368309
H -1.327728 3.202712 2.095999
C -0.077457 5.766880 0.263963
H 0.352697 5.681433 -1.844340
H -0.584331 5.536827 2.342655
H 0.245333 6.797836 0.372300
C -0.683469 -2.939333 -0.262303
H -1.165734 -2.928288 -1.253669
O -0.619321 -1.644793 0.256269
H -1.383512 -0.905235 -0.610904
C -1.538571 -3.799339 0.681331
H -1.639589 -4.820132 0.286443
H -1.042885 -3.854512 1.653273
O -2.805471 -3.232591 0.961228
C -3.708535 -3.064558 -0.038109
C -3.661778 -3.716482 -1.273037
C -4.766080 -2.193433 0.243897
C -4.664020 -3.481480 -2.213629
H -2.862694 -4.409408 -1.508850
C -5.758809 -1.974323 -0.698416
H -4.777253 -1.700517 1.209198
C -5.714161 -2.614502 -1.937459
H -4.616725 -3.991053 -3.171280
H -6.565521 -1.284358 -0.470871
H 6.977225 -0.003364 -2.184388
H 4.367900 -3.277152 -3.155075
H 6.614824 -2.213547 -3.250679
C 2.676372 2.121077 -0.624673
C 2.807806 2.891080 0.530800
H -6.489890 -2.439027 -2.675824
C 0.673590 -3.593316 -0.427036
C 0.960048 -4.368744 -1.552013
C 1.639944 -3.464359 0.571843
C 2.189557 -5.011662 -1.677888
H 0.213293 -4.466236 -2.337090
C 2.870713 -4.098905 0.444698
H 1.422644 -2.847856 1.439440
C 3.148046 -4.876750 -0.677190
H 2.400476 -5.609943 -2.559379
H 3.617963 -3.978510 1.222596
H 4.111604 -5.366883 -0.776094

[4b]

Ru -0.325820 0.184303 -1.311563
O -0.125292 2.075497 -3.631113
C -0.190756 1.386935 -2.692508
P -0.973821 1.830658 0.063143
P 2.143881 -0.024588 -0.858779
O 0.980657 0.536073 1.730729
C -1.303621 1.080242 1.703795
C -2.556102 1.007870 2.308463
H -3.412950 1.471264 1.833616
C -2.717239 0.310083 3.500939
H -3.700170 0.241074 3.953711
C -1.632213 -0.314515 4.109259
H -1.786567 -0.851520 5.038676
C -0.358148 -0.249244 3.544328
C 0.919658 -0.813767 4.169170
C 1.824685 -1.281478 3.028876
C 2.714889 -2.352740 3.093007
H 2.780938 -2.950360 3.995655
C 3.529642 -2.669451 2.008664
H 4.223774 -3.500133 2.081296
C 3.439017 -1.949929 0.821479
H 4.037181 -2.242104 -0.034657
C 2.547596 -0.881610 0.713178
C 1.794531 -0.558232 1.839283

C -0.239658 0.443478 2.343545
C 0.617630 -1.947950 5.152842
H 0.117273 -2.784761 4.656865
H -0.016811 -1.593738 5.969352
H 1.537435 -2.316059 5.614499
C 1.635687 0.335581 4.918863
H 2.570404 -0.025688 5.359234
H 0.995306 0.720917 5.718616
H 1.872229 1.159837 4.239564
C 2.925742 -1.152438 -2.079096
C 4.188594 -0.944419 -2.639980
C 2.208370 -2.309733 -2.411134
C 4.719665 -1.872609 -3.532446
H 4.760385 -0.058600 -2.382972
C 2.749192 -3.238908 -3.292793
H 1.237925 -2.481019 -1.952720
C 4.002079 -3.019403 -3.860222
C 3.316457 2.173024 -2.088911
C 4.585690 3.130020 0.192146
H 3.736981 1.434508 1.201501
C 4.091632 3.324115 -2.157074
H 2.812508 1.811845 -2.981466
C 4.728541 3.805143 -1.015075
H 5.065719 3.509310 1.088623
H 4.190692 3.849827 -3.101629
H 5.326036 4.710204 -1.065591
C -2.496616 2.777082 -0.324824
C -2.907632 3.811219 0.527300
C -3.243409 2.501201 -1.469901
C -4.059413 4.535915 0.248935
H -2.323320 4.050588 1.411292
C -4.391186 3.238585 -1.754742
H -2.936329 1.694561 -2.125594
C -4.803724 4.249827 -0.895147
H -4.373793 5.327644 0.921483
H -4.961505 3.012276 -2.649931
H -5.701847 4.818887 -1.114778
C 0.191944 3.199207 0.448887
C 0.763116 3.906510 -0.612211
C 0.476879 3.595724 1.758187
C 1.599137 4.989254 -0.367539
H 0.559692 3.615639 -1.636920
C 1.324311 4.672719 2.001334
H 0.037118 3.067372 2.597970
C 1.886905 5.371729 0.939091
H 2.041861 5.520708 -1.202970
H 1.540858 4.963730 3.024610
H 2.550885 6.209599 1.127823
C -1.305386 -2.605497 -0.409670
H -1.895976 -2.649777 -1.337481
O -0.310317 -1.639898 -0.500294
H -1.878009 0.006657 -1.630259
C -2.275874 -2.332662 0.754241
H -2.822352 -3.244834 1.027548
H -1.694854 -2.008869 1.622362
O -3.184649 -1.274591 0.503171
C -4.206657 -1.456442 -0.369946
C -4.562775 -2.675086 -0.952684
C -4.950703 -0.308915 -0.663336
C -5.647780 -2.725606 -1.828037
H -4.008972 -3.581711 -0.739564
C -6.023557 -0.374025 -1.537662
H -4.660128 0.626995 -0.200726
C -6.380970 -1.585300 -2.131254
H -5.912528 -3.676935 -2.279915
H -6.581782 0.531226 -1.758476
H 5.698489 -1.699274 -3.968914
H 2.188287 -4.136337 -3.534001
H 4.419322 -3.741750 -4.555193
C 3.197391 1.468767 -0.883789
C 3.830119 1.962104 0.257605
H -7.216837 -1.635930 -2.821029
C -0.664251 -3.965061 -0.182198
C -1.173047 -5.119305 -0.776781
C 0.444430 -4.069219 0.659739
C -0.586261 -6.359742 -0.535059
H -2.025073 -5.045205 -1.449507
C 1.032528 -5.305057 0.902324
H 0.850351 -3.165860 1.101172
C 0.518641 -6.455470 0.306646
H -0.987363 -7.249853 -1.010746

H 1.899507 -5.366102 1.554227

H 0.981698 -7.420380 0.490075

Appendix -B

SNAP coefficients

Grubbs II

Ru

2.6545791697077154E-008

-0.68998800464101184

3.4474302205342444

-8.2007248222712139

0.79062795289499921

1.6034917100083144

8.1454525433130041

-3.6157239608503247

0.89333314383634077

-6.2326317240652251

0.28173464421064309

-0.25439140565581053

-4.1658207137521579

2.1864130939554967

1.3967971140353828

-5.3363295710536134

6.3381465526814420

-0.73102592122431487

-0.39135906730611419

1.2305902035225806

-3.6555327358444401

-1.0840055680254737

3.1958676805301436

-2.1948501943453764

1.6494099205509949

-2.2561110371488970

3.3811234552493308

0.29481089323169307

-3.6690869751837649

-4.0216086418888572

4.0410737108410411

-8.0671576112167127

5.9432955066313324

-0.23273369284657622

2.4028548132504564

-2.4508485013529366

1.5600208111095140

3.2239482946050861

-5.5114132090759158

-1.7427991078144474

0.79126716954888265

2.2594177671154143E-002

0.91206201150672839

-0.65638569173264838

3.5465105181392342

-1.8952647706965038

-3.6754220615388924

-2.4196813495645348

2.3596103953851482

0.80709550972532484

-1.0814114345536321

-7.1112746077281408E-002

3.1792738034511685

-4.0265187552583273

-0.59969515271641372

0.27570251821899022

Cl

-6.0630458438922762E-009

0.96879505882656303

1.6137062118108672

2.4956928425971432

-1.3879250581943579

7.0738849969673159E-003

4.7778414395213096

-2.9942199613527540

1.1442559446762806

-0.63379886648713113

-2.3265868424238980

-4.2090103709394624

-3.9165927513344867

-1.5629285398363761

-2.0872301090581278

1.7430906710981746

-1.0010275208017259

-4.1800545099553963	-0.16584877554885377	-0.82351820400324105
-1.2016319562362321	1.0011955401297574	-3.4404009295678240
4.2656769964366283	-3.3995201215998820	1.8687868811110393
-1.1373360080023649	1.2762673892181868	-0.78354923664725407
1.3478736871056338	-4.3534690040796864	0.38305924302590505
-0.56418474514675332	-4.1888637434535880	-1.9914980361012142
-0.33989945608205657	-1.9972034661048514	1.8723264639987045
1.9819872730828885	1.2688145368737198	0.88870281755116265
0.89711253461875706	0.91794140776419142	0.11241797481539556
-0.59823161399333780	-4.3308588419256129	0.63763042854661500
-5.4163844941528776	0.97186216020310923	-0.52051648023376040
2.6097004737105300	-0.29345882829474412	-1.7578906889076109
-0.85372072516400899	N	-0.22282142408948713
4.3466616877531701	-3.3083743581552341E-011	-1.2088790630606003
-4.4541850058431205	-0.72841595534502168	-2.1476816121046123
1.9931568252148839	2.4727313512871607	3.3845909316565894
3.4186258091012314	2.2199333030885202	1.1901834109900675
-0.95165778486889163	2.6997149144255119	2.2274635627280222
-4.6817452760222329	6.9278902538680134	0.17004404067027928
-0.44243065202319320	0.67145865696174434	0.15868629547186605
-1.0996625032066580	2.9383095985398850	-5.6995569064591349E-002
-1.1109858043726808	3.1838068939478710	-1.7146568305723029
0.86044633326383957	-1.1093246427582331	-0.48165631156786903
-1.9650731330837141	1.0736082442648767	-0.15534795542316893
0.90411256383817040	-1.6275790664857210	3.2220357161505389
4.1063494268067045	0.83319273279536454	0.74369519019802566
1.2083807970772673	-2.3422867518931016	-9.6861000833445163E-002

-0.15712157990240508	-1.7736643683284941	-0.66457280232343108
-0.44273538844305027	0.50946543987686910	-0.22645772735950237
0.12322722216987525	-1.9436852379035148	-1.8458214470461183
-1.1398425427654937	-0.41724297619208811	-0.46031126924090943
-0.99884684670125456	1.2998521410218000	-0.79848435136704998
-1.6371774783546491	-9.3416065663631323E-003	0.30502388806361513
1.2417233125317555	-0.27146126186008829	0.20557214160329171
-0.25726073278289302	1.9745690025909735	9.5576013247818351E-002
0.20400943966331753	-0.79267495069798199	0.61089067792510121
0.32061506127609996	0.60388350526733769	-0.17873413369555033
9.5617642699324809E-002	-0.15403705375348184	-1.1028441054494451
-0.26263515007879940	6.4091699428562202E-002	-1.0998837408362019
-0.26966174015530064	0.49423392265202087	-0.54773822349474866
0.73290935244215771	0.59034889985642613	0.28284741840442501
0.57196577979237784	-0.31795057966083928	6.7679236459521314E-002
C	-0.47602214834488377	0.19065490585493644
3.4038745867178613E-011	0.95489926514462364	-0.30011599029156555
-0.17051207403336283	-0.90195559893376842	0.10128947798674717
-1.6533287976230875	0.65116856587478034	H
1.4012294327689057	-0.11667667991035753	2.3192688849200277E-011
0.13249519859474015	-0.48844290748478958	-3.6722734063652802
2.7619724318682741	-0.73513865326826766	2.4642507714117774
0.96555987756184569	0.53340053248142261	1.8623256217916582
4.7150654367549699E-002	0.63004872583272309	-0.24627221869107072
-0.22606020425290721	9.8037106391095970E-004	-3.5906889232503496
0.55437461399528476	-0.21054351648313674	10.395092485019303
-0.23971882385367591	1.2351155167927943	7.9316833916676721

7.2279424409842221	-1.1724845808381588	-0.72848218797089581
-5.7138899920911559	3.4134780771264728	-0.45695212651992484
-1.7679016839668278	-0.59446523120525341	0.58565764638925077
1.4429103304612818	-2.2605306554868427	-3.2301559113665941
-3.5776927810328183	-2.0785865760972615	-0.45670064229350837
-2.6173030193308877	-2.2000840194777558	1.3381045348920704
0.76023680043156161	2.2156374722843006	0.66186009382660205
-0.42117783059992564	4.4958766925044147	-0.87038712287258180
7.6277682454721720	-4.2664002381197523	2.0646759803581616
0.26299177013452224	-1.0272192656471109	-2.1781471743279295
0.64850891427486157	8.0918924480148799	0.67611686342644028
0.91522848084112807	0.58872126128270685	1.0399320431701271
-2.6505415532798624	-0.63073869509592806	-2.1606479319598306
-3.7019701888224259	2.1756602411246786	-4.1491376606899406
-3.6183607912132252	-3.8994170690697580	-2.1605165199697756
-0.44708753374955673	1.9391902564653463	-1.7920647410000454
4.7041353056969930	0.10731969834155264	-2.1129009897553881
1.2177561558358014	-7.7418300590099864	0.78535800113894472
-1.2708206990303215	0.47002437644602901	0.20559681020981044
-0.15797809021452103	2.1668620765452120	4.3442177784231290E-002
1.9633245981252960	3.1726837437007709	-0.40204429549471138
2.7100717305341102	Si	1.1980835719651686
1.2833197365112265	-2480217.7846668512	0.66317486267376191
-1.5386886102485660	3.9693263620559205	-2.2306550464851864
-4.0993254504003058	0.79911599566257729	0.96993857691573937
-2.1080727012141542	-0.65081052757047120	-0.79862261917771105
-4.1348155208963595	1.0615949832254923	-1.4938759731776285

-4.3747495179679792	3.9465257879896067	-1.8395835987855176
-3.0359333777785658	-1.1810591790072755	-0.93926533973838189
-0.46107396021898367	1.4027275129318759	2.9919041997363429
0.40105332948151867	-1.4354714757356861	3.1087971042215599
-0.72615953266969491	2.3654408177176358	1.8000339512587515
2.0299128406355105	2.5290795121754268	-2.2578024279755518
-0.56190255793389698	3.0087599304259820	-0.26706553078583894
3.1143880833716069	-1.5413944376646915	1.0005608233725121
1.1031220914034796	1.2350110997125561	-2.0088027482221373
1.5117774266612489	0.36195842257491129	2.4528357950712065
3.2945191214339773	-1.2983993651606751	4.0367932799624846
0.80894107038424634	2.0163610554207398	3.5640819882554755
1.1107124273636411	-0.62774990222391447	-2.1609221351076870
-1.2286709311291888	-0.99187090844513759	-0.11813416438643325
-9.5651812137545492E-002	-0.40289136972485357	-0.62891718004245023
0.21918117986619076	-4.0199581136305822	-0.56432033099274170
-3.9646615243330459	-0.83128876695739518	0.21690097138625911
-0.91117712900107806	-3.7590672070040090	1.0263411487338669
-3.9218856111079912E-002	-3.7077685100072397	-1.4274158868828293
0.83081696560654983	1.1978292954383427	1.6819685726944087
3.5502478187164690	-0.69204805338000785	2.9230147282411894
-2.9283268602259191	0.36288393459095930	-1.1476077390367456
0.62371652137083633	-0.36880992579684030	0.24283045375574053
2.2725483399069422	-1.9064629702993245	-0.66291834760030033
Pd(PPh$_3$)$_2$	-0.32316491870173103	-1.0732884409280026
Pd	-2.3160727718326890	-0.49742008105811375
-5.9471901215220758E-008	3.1020446178109999	0.37090599506517025

-7.4947440088501960E-002	-6.3363862508790936	1.8081030322373193
Br	-2.8943147228852082	3.3803164845480218
5.7090883500398660E-009	1.6574322937792612	-4.8243558464063341
0.16117776329595246	-1.7360235569326596	-1.1405312116270556
0.94062579501241206	-1.9619349427133201	P
1.8813215669689836	3.0545682280158513	-9.3612400336570217E-011
-1.8345379461784632	-2.1837784791342245	2.4196475403526598
-2.2329564171939102	5.8847658709952064	3.8418094531324081
5.5049736572035926	0.48887621652849611	0.31748201633856776
1.2711048834668373	0.70865985721567326	2.4440359748811407
1.3138038482607841	-1.6098489734798853	-0.20670635112602437
-1.9220625607455291	1.0349478651380353	0.64843947511407840
-0.31327942663587521	1.7274502877578097	5.8535983446526361
1.9201932680635623	1.0658183303678423	-0.68023265044203018
1.3503706710578944	2.6410349666186281	-2.3127725523602760
-0.38281696071271565	0.47688372361832271	3.1781760840828852
2.4856000988397788	1.5909208706170861	-1.1105023868993478
7.8174987462665088E-002	3.0680685172447437	-0.59178825923852851
-6.0992366376188496	-2.0385004041653789	2.7016856007249341
3.7838922041074174	-1.4596770958252794	-0.66872488706413780
1.2261091526733432	1.8612421843124658	-2.0638395248450108
-3.3183788623636037	3.9570337121431001	1.5265513335227796
-2.1528690057881965	4.4753487252834265	2.6592675637907446
1.0733382962405706	-0.23549685739636508	-0.15722661971456298
-0.47915540126754225	1.8573343495087189	2.2784776917628640
4.5347490371730474	-0.19844971733549005	1.8145912740403192
-1.1733097906105696	-0.96554237880489380	1.2074902754297145

-0.57763322623506652	2.6008433447256336	0.17009797575075347
-0.36668465620825352	0.72165807049042674	1.2285370666662827
0.11860260087305505	-0.97200882907694042	0.13380897623246371
1.1611077400367134	-1.0845568645378394	-0.14057092510211985
-3.0990675200701405	0.82848339902569967	0.60582115272038950
-2.1018633255859482	0.40167371548482911	1.1162948537735187
2.2063265298608230	-0.12400319861666961	0.27520190649669174
0.84716405371136372	C	-0.21783157261091507
-1.3340499730243169	-5.0336156801742355E-011	0.96850592841709471
3.7812776258612337	-0.51801205689945962	5.9911222765942053E-002
8.7470911395432810E-002	-1.5763516409937408	1.2828828992823615
-2.1827634649270031	-0.26084301096426238	0.16985201635075581
-0.32282292286333891	-0.49106211050843795	-1.2046020958216948
-2.3969124974275595	-1.0653357947473867	-0.28488388911331397
1.4128946873954444	1.0577360762692223	1.1185533538360217
0.98479669691525062	-1.5373730494982805E-002	1.1818417989648384
2.3344754781760098	-0.74946652187429330	0.62879002385955740
-0.44772904971498045	0.35931764354905110	-0.13064583708541172
4.6155086694276424	0.29716052437313312	0.39738418269086795
2.2960915578003913	-0.43305747395989619	-1.0243304599204501
1.0122148285898767	1.5731931414310483	-0.18682863154473645
-1.3859090949222876	6.7785451973001787E-002	-2.3432881069138118
0.75764380210925741	-2.9515791435417455E-002	-0.87339721428526507
1.4469027249022042	1.6866638926404420	-1.0532628031570721
2.1473082321686592	1.9795219916094967E-002	0.46793290826531886
5.8993241328693387E-002	0.33558566673922313	0.41185601329035382
2.5030835287631783	2.7532328942020925	0.41561631555465883

0.26569142966161546 4.7546722928880261 -6.5041382393835692

-0.25219434512752348 -5.1091533034376813 -0.99315004583902677

-0.90893980310092748 2.5326091235363428 0.71351263776221685

-1.0732097313266353 1.3385556303233941 4.9945425599184343

-0.30327282334027539 -7.6928970963500459E-002 1.9059544397778634

0.32224552732868317 0.41870267029418878 3.1132386510979568

0.24878928719569909 -2.7155991781922588 -5.6773493885291773

-0.34787755805044723 0.69101427522373937 4.1016642158096204

-0.45390031983931006 9.4666263623615841 -4.4429522738525611

0.17886290567150384 -1.6608251211721172 -4.2070583437588791

H 9.8771587084359176 3.4308854990309499

-43748.403819293038 -0.56090315293360749 2.4156285852656385

1.2833855257473770 -2.4844700131434103 1.5292796636167996

1.8977574447451750 -1.0725531803673574

4.8283921202437634 -0.58127591287992686

8.2578529381558710 -2.9238909136829356

-9.2061996355272200 -0.37487362610326558

15.006660242564024 3.0095776283388513

4.4403641117338086 -0.62282621581511022

3.5046239477843120 -0.86398319972625970

2.8820596048084348 -4.9054693973460433

-1.7698691283983596 1.8336469152798438

5.1632690480510472 0.24171610086490883

-3.3272487251160197 -2.3051079806353676

-5.7603442221738117 -5.3763128504037683

-2.1578591259713025 1.2066942466605246

-8.3491491197738767 0.93959905435865654

Xantphos

Ru

3.2388483096857619E-008

414.18952304214315

531.61520900926075

-151.99595664887426

104.15777916082395

285.25858232929022

-316.11240976880225

-558.76834036159050

46.042081832449909

-135.15560129194211

269.70749615416071

50.323360482315124

886.86888552284063	-134.80798908418052	71.718559925013039
-501.52750202510811	-10.191291650462993	38.595636805945816
376.14188837203500	-340.89043453797274	4.7211878919493797
-194.59940900246869	-266.25041079508253	6.1194906559236788
-729.75299936744375	-520.07522157968640	16.293040818058557
-178.93983978746829	177.41411099105895	47.430665942522687
-227.14677873178329	841.94609282829549	133.23884097432182
-1152.8388691279326	-20.464630070614700	28.114569597153718
186.96576846384616	88.319136571512075	-20.483447283839133
-58.617257552718044	336.36406141289427	-78.399875072618343
-228.03516807449330	-253.92960383302642	-156.32039920448454
-34.801409424185671	679.53576313133203	32.354117311866226
65.632127211639585	-193.81513928181639	-11.899564713464567
238.82519267276209	308.64737189603670	59.356344710303318
-769.57857071224339	-262.06936154730175	14.451580837054980
28.634428023156953	378.92393689985516	-117.18943733918594
-505.44813286317503	50.568139121741318	102.45229535513997
167.80163713058306	O	-76.017173964225265
426.47450101717237	1.8386919101396986E-009	100.94408404139054
-85.968760767915512	-66.894613918652894	-99.266834503808440
-381.50319902853931	80.103842294859689	-19.845989416738895
61.184166904220874	-17.918129255024287	-130.52445156939703
-121.03406633764443	90.192458727960371	81.572450830474537
112.81943786395009	-145.36667280684767	-43.828444793143227
-60.586013995087683	-73.468479654619330	-21.894472045732847
515.09906281263397	58.403516397839951	-70.409518039644553
50.806307183594434	55.745882960620797	-61.525315730601662

-83.589551205158088	-635.82690326236082	34.159912346998766
-5.8243059038573204	-671.13981328131240	-171.88744222159707
-33.804850374702042	296.88351681659071	31.434561263017798
-69.330214793505235	34.114923250785608	62.011181118466546
70.745374013727456	-31.618020173010812	-422.46274661912594
63.315492466845242	65.058614584460855	30.870363122743289
69.975842540385386	-60.541892613144988	166.61482849514076
15.495312807800120	8.4067674234056913	31.040349906714059
-13.534172646010237	-9.3056438949174893	136.55773452599706
-62.954838284086328	-197.64746127627524	251.74921144132009
-21.107845920884078	-582.76319262266838	66.557851753965608
-5.6688654000408123	273.85576166683092	-114.14380195795701
53.934706711940535	156.46673404072007	164.20639410599318
87.435762834526798	14.078955300054554	-136.56650322997845
30.536138257919657	-67.551221588345058	49.896028994924500
-6.9361989596059788	-44.451528572619019	-92.272020917903490
41.865215979368642	86.372824411203965	96.466928981681761
-17.873007028187910	124.33363049541400	75.538718701998107
29.069259068713002	-146.16281437553744	-41.318664808043778
3.1005848040573132	208.55874067763463	65.897989201638367
P	344.56165242391648	-36.051803863272177
3.2732816262711539E-009	-534.69015433429342	189.95819414189316
-222.46812662299715	-65.900405647667455	95.311247837534751
290.76098369018308	357.88252269765883	C
233.43069923586080	51.192418908629470	9.4243737728374013E-008
-224.25960960061883	-97.092697521867393	-7.4169777425224854
-401.19594786352940	-189.48912220310993	-11.702736344245151

27.639319264173533	6.5486011886946622	-44042.021427004249
39.499443463066619	-14.040490436682507	1362.9321449278953
58.339960381461907	4.1065545369229088	-635.88056510656656
-18.540297533016407	-4.0206916048153003	512.25932900580870
-8.6344061632274780	-10.573993718791892	614.99523958847271
11.064830533344002	28.568117916670030	-249.52121229501421
28.644526804813225	-38.408590235711415	-128.59744152102621
-20.299843585595898	27.182045645547209	-407.87191439264410
-47.820430275107903	-4.1645250941277698	159.62356965752247
-12.409793977801311	-14.885339157037466	55.617568372257516
-5.2828166005275703	-8.3049038775253941	60.945067337532166
5.9392227741778925	-1.7284553879791493	-30.510543572963090
-0.25325107539487007	6.5182939355144249	-262.66885692526699
12.041454764056294	-1.6406236687248288	-670.06348924044210
-41.496328420801213	0.27741977548916108	-628.11925483449022
-3.4636922580414207	-1.2998316144023936	125.53259946258960
10.708386435783677	-13.433939372610622	-74.848731873062647
-3.5054117963612406	8.1111196894403754	-139.54752111354856
5.1263565421419957	-0.87837498208260012	-21.164760176433632
-6.1315083173306490	-5.9841833019760964	98.803399040982868
2.0590926155275882	-8.4049917971561907	482.02373933666405
-3.8874540923856213	4.0908265792231679	544.57978435284952
18.891451218568893	3.9957989454228238	-110.86745966751033
-32.533182767323360	8.1738404467140811	-91.448262736900872
19.246625555616792	2.5409155183272500	173.99146211200394
-6.4497939009698486	-5.0813841045942851	-573.11971019925102
-4.7140597698535336	H	78.816133259514686

257.97878791236343

13.971216198709568

-158.52510493066865

-333.27021358075893

73.137747920246767

184.28957252602115

-384.12817663335636

378.88161516623103

153.74932114401466

132.58228691619516

12.505357969185326

-59.834416326785828

320.86989964052583

318.41155658047404

-697.84359758572782

166.39856297770953

-191.57941571102015

-438.00137293656013

-307.58454616891879

569.26326099646974

-143.44652379004430

-164.09443119398836

105.35993752129620

252.51664044597101

293.11784862661119

265.52400663511202

-485.48036922359302

1.2738480599847193E-002

-431.61229823895201

PEPPSI

Pd

7.9804082645622645E-008

1.5812988261815240

-1.9274667461484691

1.6127496902180611

-1.2187855415992956

4.6128539348030397

3.1301428761117847

2.5954012463307208E-003

1.4915074979109186

0.95048539781425478

3.9764387130413414

-0.12107646155112232

-0.36898729779707912

-2.8154328984566397

-0.63894558196820206

-9.8005644971531098E-003

-3.1198533169729163

-0.24147696076098396

-1.8866881521812811

-2.4670864929865437

-0.48488305199778658

1.7841956461655373

1.2411564608030647

0.79157426635676809

-0.26654556270168189

0.56082652654837861

-0.66792479285719053

0.23753364637185070

-0.72944787133775468

-2.1637355773256113

0.70088836394622123

-2.0536912321744092

0.67451732241744589

-1.3244324852497700

1.7018955632049182

2.1879709476513844

0.54178681716869459

1.1360982431734392

2.7630128871277311

2.3790723543677577

-0.19338288712583793

8.6141709123474727E-002

0.63583558457385314

-0.21170343839162689

1.0929365755009950

-0.88821750605293981

-1.9551472463081281

1.6786284767854467

4.3194707192494715

-0.61053713594300985

0.35217390925399933	2.5033443927238936	0.17804881076113604
-0.74620443245180290	2.8009291587632741	3.0480063288421566
-0.45242876945670002	1.0922059944467790	1.3470538811486417
-0.69143535648140775	1.7288605182723060	-0.62471227529434303
0.41548686572781351	-3.4298922303985542	-1.0381569573531841
-4.9193664902345245E-002	-2.6024069332036230	-0.35439353976338739
N	-0.26446125614118410	-1.9760743360604849
-8.9124923537214720E-009	-0.36716515954704693	3.0158650951787815
1.2851409925201887	2.8096057218258315	-1.1669062990368779
3.7423036746762106	0.89693348651989147	O
0.49116072313707038	2.7210667026103934	8.3816328226512490E-011
1.1265775402924141	-1.1552892842854792	0.25242860080205864
-1.0958007571769730	0.77317274749608977	-0.94486487086015181
0.84899690378957815	-3.0281284389224128	-6.7900800737496887
-1.2843642664059731	-1.6873537301033843	0.41910469832977537
-0.67338173224365017	0.56230373188830673	-3.5519200814363723
-2.5263429726433992	-1.9390326056658691	1.7695903352414313
-0.92378213207693261	6.2691809102475373	-0.23286198703841360
-1.0848159345701096	1.9160212176760161	-5.9741300091812923E-002
-3.8441636073208891	5.5552312945926543	-0.14180165126575064
0.29286984716631553	2.1370847837084703	3.0408318842738029
-1.4856418693287843	2.3411338617047832	-3.7917434529662795
1.3063455376337827	2.8008064037027323	-0.23723951838733828
-0.54343864600709990	-0.26762870606432942	-0.69688128315606379
-0.73547870041363306	-1.8148036186812240	0.12419902880694855
-1.5516733165409080	0.55871617681625885	0.28718576970804793
-2.8121284753069995	0.55836405263583422	1.6085019879970417

-1.8225383221140130	-9.2685478566935639E-002	-0.47817316886263844
6.2921265756071543E-002	2.8979788402868558	-0.72183619709091362
-1.9145121872620281	1.5821665988710647	0.23467527831249227
6.7747167943279257E-002	-0.62936340319621875	-1.8751071843843271E-002
1.0842540113895756	6.6265187045109822E-002	1.2841187161463901
-0.10130002187094693	0.55896832143742725	0.28206002122562096
0.39385951984097495	0.14617036836218081	1.2728213701117810
1.3474049636555081	-0.23113599179281435	5.2348506617257998E-002
0.77129120212113167	0.26815942846497515	-0.29826183629114450
-1.3029534677471792	0.10550805745427541	-4.8074960264429888E-002
0.20205206120997948	0.43862565986877933	-0.20770865752996487
-0.82580129418180126	0.29067938747824307	-0.94229673043541484
-1.1736895365555458	C	0.28519482956367898
-1.4794106104400513	1.0188455296943111E-010	-0.79778501172951977
0.93984418625572930	-6.6909419955818908E-002	0.50823260168325657
0.17651686755628401	1.5856104256868864	1.8787662571300034
-0.70745639202785859	1.9619714819434988	-8.3096436694146902E-002
-4.3879686091578197E-002	0.38324720864170125	-0.11220857004927538
1.5914914433780325	0.71419560504173096	-0.49161095139588318
-0.98507810110590766	0.89856943945722245	0.36043946881362199
1.7822490206128339	0.17671601495463818	-0.23927214803349259
0.66438154636451852	-0.37286962469133805	-0.59311279789051219
1.4690009844189724	-1.0793944534541586	1.4599766859905680E-002
1.1139261348458105	2.1391632660088158	-0.87019489243022785
0.66895159133452020	-0.12230782375829818	-4.4985390957974443E-002
0.71728806436524950	2.5254009795864958	-0.30000616290814336
0.10922738793778052	0.23325479001164534	-0.72582997516646552

-0.25533058833918154	-1.1761840378348354	1.4034386735539521
-0.33552309534718544	-1.3444571358725073	1.1221501209019793
0.23499223729053831	-0.51584867260085898	1.9881083476926327
-0.10975090757786995	-9.1307221045100237E-002	0.24660454645828192
-0.27911466794729445	9.6306051901914227E-002	0.34539744941369843
-0.45931354884249198	-0.38137830537675615	-0.42848976824315821
-0.10639418082488510	-0.29316773285479164	-0.65171716553685477
-0.36335213046734033	-0.88731418381920202	-0.44368772639135695
-8.7210825651411306E-002	0.20553350797875580	4.8707951820419475E-002
-3.2508163783854647E-002	-0.52543681548280596	0.83951705706370994
0.21907112438118909	0.68124920758308549	0.62728280691351646
-0.17728035184152788	0.24581044747724901	0.47867653141851652
-8.2427954798288933E-002	-0.48906971547086009	-0.12876554411266694
-2.3573996002826759E-002	-0.50725079405015183	-0.11155446810437093
-0.13754590221722771	0.20996239832344904	-0.41336994854957015
H	0.30368339440004111	0.12740405837271926
-43752.089576633232	1.4370170499659829	-4.4925537479698241E-002
0.14743956668017552	0.34746756056149519	-3.3369977038059717E-002
0.21333576961720691	0.28038610895211813	
-0.66928636130314101	2.1455384998487652	
0.28661570433496020	1.1876935459279796	
-0.97490929586705855	0.70488495332003132	
-6.4639866954630337E-002	-0.54083147977929502	
-0.79494758588211833	-0.66333266824275816	
0.34754960330991064	-0.13373306303078017	
-0.29593172711632237	5.1827638458808938E-002	
-0.36270391038140476	1.2243901756878219	